

Replacing the BO in BODIPY: Unlocking the Path to SBDIPY and BIDIPY Chromophores

*André Korzun, Stefano Crespi, Christopher Golz and Alessandro Bismuto**

Table of Contents

1.	General information	1
2.	Synthesis of dipyrin scaffolds	2
2.1.	Synthesis of dipyrin scaffold L1	2
3.	Synthesis of SBDIPY complexes.....	3
3.1.	General procedure for the preparation of SBDIPY complexes	3
3.2.	Synthesis of cationic SBDIPY-1 ⁺ -Cl.....	5
4.	Synthesis of BIDIPY complexes	6
4.1.	General procedure for the preparation of BIDIPY complexes	6
5.	Spectroscopic Studies	8
5.1.	General procedure	8
5.2.	Evaluation of solvents	9
5.3.	Analysis of the decomposition process.....	10
5.4.	Determination of molar absorption coefficients (ϵ).....	17
5.5.	UV/Vis spectroscopy of SBDIPY-1-F	23
5.6.	UV/Vis spectroscopy of BIDIPY complexes.....	24
5.7.	Fluorescence spectroscopy	25
6.	Theoretical Analysis	31

7.	NMR spectra.....	32
8.	Single crystal X-ray diffraction analysis.....	43
8.1.	General.....	43
8.2.	Comparison of geometric features in solid-state.....	43
8.3.	Refinement details.....	45
9.	References.....	63

1. General information

All experiments were carried out in a glovebox (LABmaster sp, MBraun) under an argon atmosphere or using standard Schlenk techniques. Tetrahydrofuran, dichloromethane, pentane and acetonitrile were collected from a solvent purification system (MBraun MB-SPS7), degassed through freeze-pump-thaw cycles and stored over molecular sieves (3 Å) prior to use. Benzene and hexane were dried over sodium, *o*-dichlorobenzene was dried over CaH₂, and were distilled and stored over molecular sieves (3 Å) prior to use.

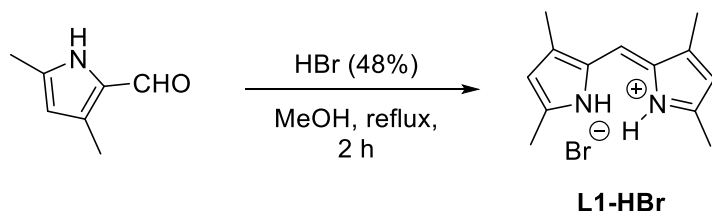
Unless otherwise specified, all reagents were used as received from commercial suppliers (ABCR, AcrosOrganics, Alfa Aesar, Sigma Aldrich, Thermo Fisher Scientific). All pnictogen halides PnX₃ were purified by sublimation under reduced pressure and stored under Ar atmosphere prior to use. Sodium tetrakis[3,5-bis(trifluoromethyl)phenyl]borate Na⁺[(CF₃)₂C₆H₃]₄B⁻ (NaBARF₂₄) was synthesized according to literature.^[1]

¹H, ¹⁹F, ¹⁹F{H}, ¹¹B{H} NMR as well as ¹³C{H} NMR spectra were recorded in CD₂Cl₂ or THF-*d*₈ at 25 °C using a Bruker AV-400 and AV-500 spectrometer. ¹H NMR was reported as follows: chemical shift, multiplicity (s = singlet, d = doublet, t = triplet, q = quadruplet, and m = multiplet), coupling constant (*J* values) in Hz and integration. Chemical shifts (δ) were reported with respect to the corresponding solvent residual peak at 5.32 ppm for CD₂Cl₂ and at 1.73 ppm for THF-*d*₈ for ¹H NMR. ¹³C NMR spectra (¹H-broadband decoupled) were reported in ppm using the central peak of CD₂Cl₂ (53.84 ppm) and of THF-*d*₈ (25.37 ppm). UV/Vis spectra were recorded with a JASCO V-650 spectrophotometer using a 10×10 mm quartz sample cell sealed with a J. Young valve. Fluorescence spectra were obtained with a JASCO FP-8500 spectrofluorometer using a 10×10 mm quartz sample cell sealed with a J. Young valve. Both machines were connected to a Julabo F250 circulation cooling system.

2. Synthesis of dipyrin scaffolds

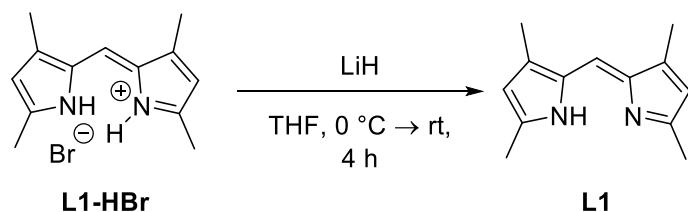
2.1. Synthesis of dipyrin scaffold L1

Starting from 2,4-dimethyl-1*H*-pyrrole-3-carbaldehyde, **L1-HBr** was prepared based on the procedure described by Yutanova *et al.* (Scheme 1).^[2] The hydrochloride analogue **L1-HCl** was prepared according to literature.^[3]



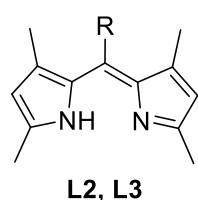
Scheme 1: Synthesis of **L1-HBr**.

In order to obtain the free base **L1**, the halide salt **L1-HBr** (1.0 equiv.) was treated with LiH (4.0 equiv.) in THF at 0 °C, warmed to room temperature and stirred for 4 hours. The crude reaction mixture was then filtered over Celite[®] and the solvent was removed under reduced pressure. The obtained solid was redissolved in hexane and filtered a second time over Celite[®]. Dipyrin **L1** was obtained as a yellow solid in quantitative yield after removal of solvent under reduced pressure (Scheme 2).



Scheme 2: Synthesis of dipyrin **L1**.

Spectroscopic data (¹H and ¹³C{H} NMR) of ligand **L1** were in agreement with literature.^[4]

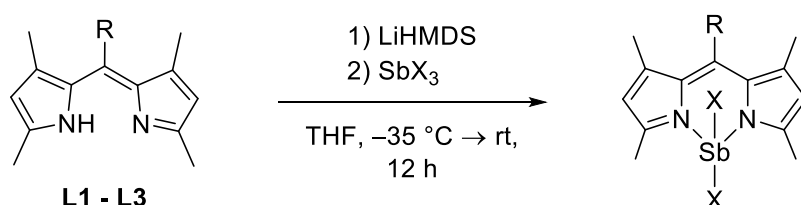


Dipyrin scaffolds **L2** (R = phenyl) and **L3** (R = mesitylene) were prepared by acid-catalyzed condensation of 2,4-dimethylpyrrole with the respective aromatic aldehyde, followed by subsequent oxidation with 2,3-dichloro-5,6-dicyano-1,4-benzoquinone (DDQ) or tetrachloro-1,4-benzoquinone (chloranil) as described in literature.^[5,6]

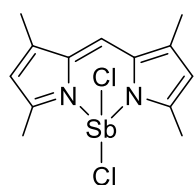
3. Synthesis of SBDIPY complexes

3.1. General procedure for the preparation of SBDIPY complexes

Complex synthesis was performed using a halide precursor SbX_3 (see Scheme 3, where $X = \text{F}, \text{Cl}$ or Br). A THF (0.1 M) solution of dipyrin ligand **L1-3** (1.0 equiv.) and LiHMDS (1.1 equiv.) was added dropwise to a pre-cooled THF solution (0.1 M) of antimony salt SbX_3 (1.15 equiv.), resulting in an immediate change in colour. The reaction mixture was allowed to warm to room temperature overnight, resulting in the formation of a crystalline precipitate. The solvent was decanted off and the crude product was washed with hexane, followed by pentane and dried under reduced pressure. The crude product was then redissolved in CH_2Cl_2 , filtered over a glass fibre filter and dried under reduced pressure, giving the final **SBDIPY** product as a solid.



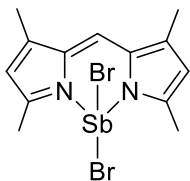
Scheme 3: General reaction scheme for the synthesis of **SBDIPY** complexes ($X = \text{F}, \text{Cl}$ and Br).



SBDIPY-1-Cl: The compound was prepared following the general procedure starting from **L1** (70 mg, 0.35 mmol). The product was obtained as a red solid (134 mg, 98% yield). Single crystals suitable for X-ray analysis were grown from a saturated solution of THF/hexane at room temperature. *The compound is stable for months in the glovebox freezer ($-35\text{ }^\circ\text{C}$) both in solution and in solid-state. No decomposition was observed by NMR upon exposure of a solid sample to air (24 h) in the absence of light.*

$^1\text{H NMR}$ (400 MHz, CD_2Cl_2): δ 7.38 (s, 1H), 6.37 (s, 2H), 2.67 (s, 6H), 2.42 (s, 6H);

$^{13}\text{C}\{\text{H}\}$ NMR (126 MHz, CD_2Cl_2): δ 157.3, 148.6, 130.4, 123.0, 120.2, 16.4, 12.4.



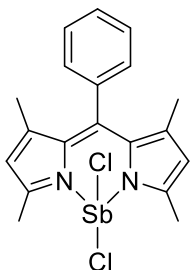
SBDIPY-1-Br: The compound was prepared following the general procedure starting from **L1** (15 mg, 0.075 mmol). The product was obtained as a red solid (32 mg, 91% yield). Single crystals suitable for X-ray analysis were grown from a saturated solution of THF/hexane at room temperature. *The compound is stable for months in the glovebox freezer (–35 °C) both in solution and in solid-state.*

¹H NMR (500 MHz, CD₂Cl₂): δ 7.39 (s, 1H), 6.39 (s, 2H), 2.63 (s, 6H), 2.43 (s, 6H);
¹³C{H} NMR (126 MHz, CD₂Cl₂): δ 157.3, 149.1, 130.2, 123.0, 120.4, 16.0, 12.4.



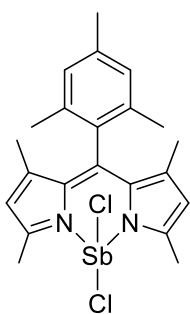
SBDIPY-1-F: The compound was prepared following the general procedure starting from **L1** (16 mg, 0.08 mmol) and SbF₃ (14 mg, 0.08 mmol). The product was obtained as a red solid (27 mg, 94% yield). Single crystals suitable for X-ray analysis were grown from a saturated solution of THF/hexane at room temperature. *The compound is highly oxygen and/or moisture sensitive and decomposes rapidly upon exposure to air and needs to be stored under inert conditions (–35 °C).*

¹H NMR (400 MHz, CD₂Cl₂): δ 7.19 (s, 1H), 6.21 (s, 2H), 2.60 (s, 6H), 2.33 (s, 6H);
¹⁹F{H} NMR (377 MHz, CD₂Cl₂): δ –77.1 (s); **¹³C{H} NMR** (126 MHz, CD₂Cl₂): δ 158.4, 145.6, 132.6, 122.4, 119.4, 16.4, 11.9.



SBDIPY-2-Cl: The compound was prepared following the general procedure starting from **L2** (55 mg, 0.20 mmol). The product was obtained as an orange solid (75 mg, 80% yield). Single crystals suitable for X-ray analysis were grown from a saturated solution of THF/hexane at room temperature.

¹H NMR (500 MHz, CD₂Cl₂): δ 7.58 – 7.53 (m, 3H), 7.39 – 7.34 (m, 2H), 6.28 (s, 2H), 2.71 (s, 6H), 1.42 (s, 6H); **¹³C{H} NMR** (126 MHz, CD₂Cl₂): δ 156.3, 151.1, 145.8, 136.2, 130.0, 129.9, 129.7, 128.8, 123.0, 16.4, 16.2.

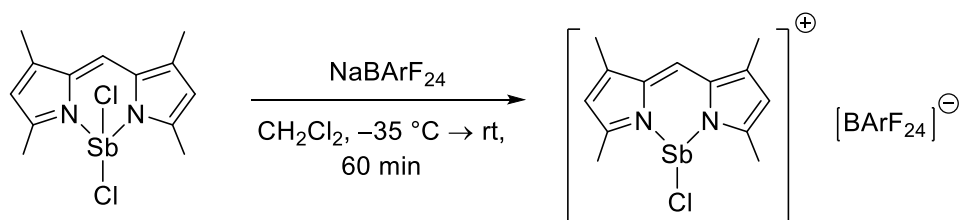


SBDIPY-3-Cl: The compound was prepared following the general procedure starting from **L3** (51 mg, 0.16 mmol). The product was obtained as an orange solid (55 mg, 67% yield). Single crystals suitable for X-ray analysis were grown from a saturated solution of THF/hexane at room temperature.

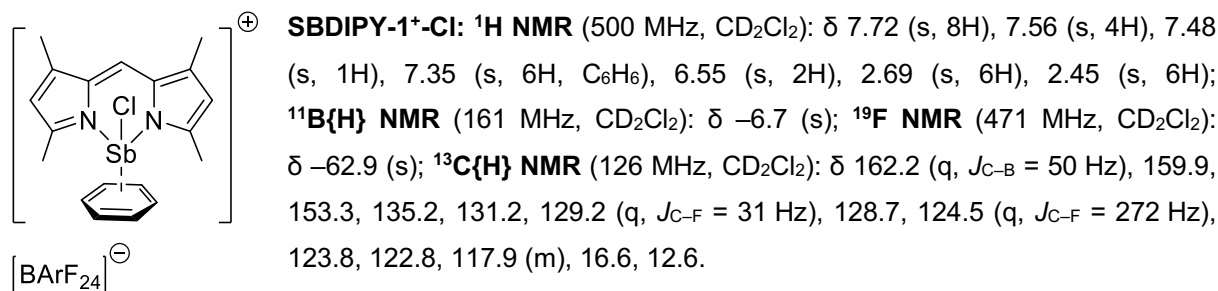
¹H NMR (500 MHz, CD₂Cl₂): δ 7.00 (s, 2H), 6.26 (s, 2H), 2.69 (s, 6H), 2.34 (s, 3H), 2.10 (s, 6H), 1.42 (s, 6H); **¹³C{H} NMR** (126 MHz, CD₂Cl₂): δ 155.5, 149.7, 145.9, 139.8, 135.4, 132.4, 129.8, 128.8, 122.5, 21.3, 19.4, 16.0, 15.5.

3.2. Synthesis of cationic SBDIPY-1⁺-Cl

To a solution of **SBDIPY-1-Cl** (20 mg, 0.05 mmol, 1.0 equiv.) in CH₂Cl₂ (1 mL) a suspension of sodium tetrakis[3,5-bis(trifluoromethyl)phenyl]borate (50 mg, 0.06 mmol, 1.1 equiv.) in CH₂Cl₂ (2 mL) was added at -35 °C, resulting in an immediate colour change from light red to dark red (Scheme 4). The reaction mixture was allowed to warm to room temperature and after one hour filtered over a glass fibre filter. The product was obtained as a red solid (54 mg, 0.04 mmol, 86% yield) after trituration with benzene and pentane and removal of solvent under reduced pressure. Single crystals suitable for X-ray analysis were grown from a saturated solution of CH₂Cl₂ and benzene at room temperature.



Scheme 4: Synthesis of **SBDIPY-1⁺-Cl**.

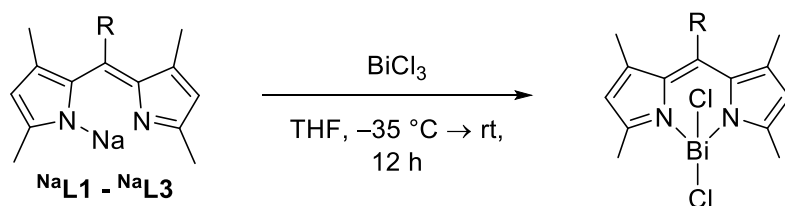


4. Synthesis of BIDIPY complexes

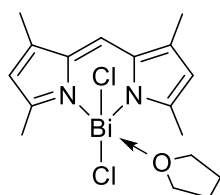
4.1. General procedure for the preparation of BIDIPY complexes

Following the procedure previously reported by Ali *et al.*, dipyrrens **L1-L3** were converted to the respective sodium salts.^[7] A solution of NaHMDS (1.0 equiv.) in Et₂O was added to a solution of **L1-L3** (1.0 equiv.) in Et₂O at -35 °C resulting in the immediate precipitation of a brightly coloured solid. The solid was filtered off, washed with hexane and dried under reduced pressure. The obtained sodium salts ^{Na}**L1-NaL3** were immediately used in the next step, without further purification.

BIDIPY complex synthesis was performed starting from BiCl₃ and the sodium dipyrinato salts ^{Na}**L1-NaL3** (see Scheme 5). The respective dipyrinato salt (1.0 equiv.) and BiCl₃ (1.0 equiv.) were separately suspended in THF (0.1 M) and cooled to -35 °C. Dropwise addition of the ligand to BiCl₃ caused an immediate change in colour. The reaction mixture was then filtered over a glass fibre filter and allowed to warm to room temperature overnight, resulting in the formation of a crystalline precipitate. Subsequently, the supernatant solution was decanted off and the product was washed with hexane and dried under reduced pressure to yield the respective **BIDIPY** complex as a coloured solid.

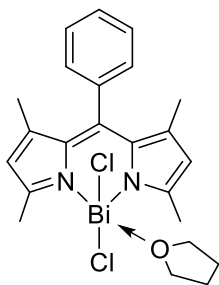


Scheme 5: General reaction scheme for the synthesis of **BIDIPY** complexes.



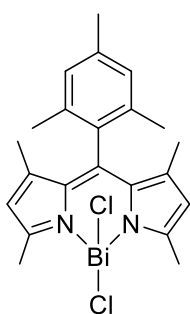
BIDIPY-1-Cl: The compound was prepared following the general procedure starting from ^{Na}**L1** (30 mg, 0.20 mmol). The product was obtained as a dark red solid (61 mg, 94% yield). Single crystals suitable for X-ray analysis were grown from a saturated solution of THF/hexane at room temperature. *The compound is highly oxygen and/or moisture sensitive and decomposes rapidly upon exposure to air and needs to be stored under inert conditions (-35 °C).*

¹H NMR (500 MHz, CD₂Cl₂): δ 7.14 (s, 1H), 6.41 (s, 2H), 3.72 – 3.65 (m, THF), 2.54 (s, 6H), 2.42 (s, 6H), 1.85 – 1.78 (m, THF); ¹³C{¹H} NMR (126 MHz, CD₂Cl₂): δ 160.2, 147.6, 132.8, 124.8, 121.2, 68.2 (THF), 26.0 (THF), 17.6, 12.2.



BIDIPY-2-Cl: The compound was prepared following the general procedure starting from **NaL2** (50 mg, 0.17 mmol). The product was obtained as a red solid (65 mg, 70% yield). Single crystals suitable for X-ray analysis were grown from a saturated solution of THF/hexane at room temperature.

¹H NMR (500 MHz, CD₂Cl₂): δ 7.55 – 7.46 (m, 3H), 7.37 – 7.31 (m, 2H), 6.27 (s, 2H), 3.72 – 3.60 (m, THF), 2.58 (s, 6H), 1.87 – 1.77 (m, THF), 1.47 (s, 6H); **¹³C{H} NMR** (126 MHz, CD₂Cl₂): δ 159.9, 150.5, 147.5, 137.9, 133.5, 129.5, 129.4, 129.3, 124.4, 68.2 (THF), 25.9 (THF), 17.7, 16.3.



BIDIPY-3-Cl: The compound was prepared following the general procedure starting from **NaL3** (40 mg, 0.12 mmol). The product was obtained as an orange solid (53 mg, 80% yield). Single crystals suitable for X-ray analysis were grown from a saturated solution of THF/hexane at room temperature.

¹H NMR (500 MHz, THF-*d*₈): δ 6.98 (s, 2H), 6.28 (s, 2H), 2.65 (s, 6H), 2.32 (s, 3H), 2.14 (s, 6H), 1.43 (s, 6H). **¹³C{H} NMR** (126 MHz, THF-*d*₈): δ 158.9, 148.9, 147.7, 139.6, 137.0, 135.3, 132.6, 130.0, 123.6, 21.4, 20.3, 16.7, 15.7.

5. Spectroscopic Studies

5.1. General procedure

All measurements were conducted following the standard operating procedure reported below.

The stock solutions (0.5 mM) were prepared in an Ar filled glovebox. The stock solution was immediately diluted further to a 17 μ M solution in a cuvette sealed with a J. Young valve. For the decomposition analysis, measurement samples were prepared using pre-cooled solvent and UV/Vis-absorbance spectra were recorded on a Jasco V-650 spectrophotometer over the time course of approximately 19 hours. UV/Vis-measurements for the estimation of molar absorption coefficients (ϵ) were carried out in CH₂Cl₂ at 5 °C for sufficiently stable **SBDIPY** complexes. Respective molar absorption coefficients were determined via linear regression analysis by plotting the absorbance of a quintuple dilution series against the sample concentration. All spectra were recorded using a continuous scan mode at 400 nm/min in a range from 700-300 nm in data intervals of 0.5 nm. The UV/Vis bandwidth was set to 2.0 nm.

Fluorescence emission was measured for each complex in CH₂Cl₂ at given concentration values. All emission spectra were recorded at 200 nm/min in data intervals of 1 nm using the following settings: excitation wavelength at 460 nm, excitation and emission bandwidth of 5 nm and 50 ms response time.

5.2. Evaluation of solvents

A preliminary evaluation by UV/Vis spectroscopy of **SBDIPY-1-CI** was conducted with a selection of solvents (Fig. 1). Wavelengths of absorption maximum with respect to the solvent are given in Table 1.

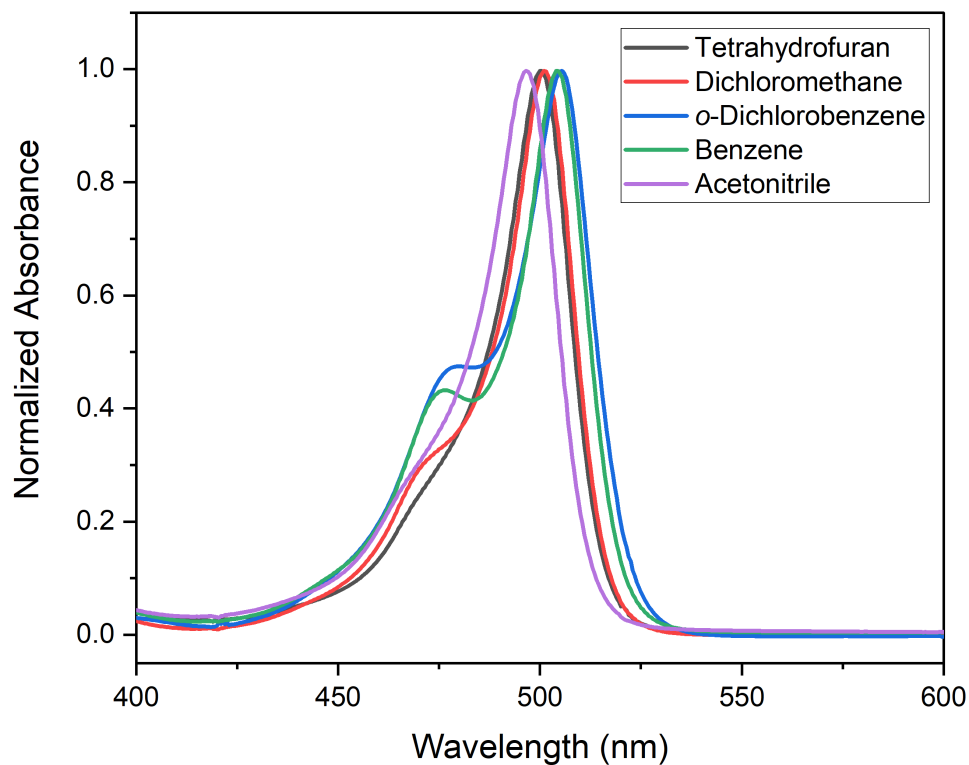


Figure 1: Normalized UV/Vis absorption spectra of **SBDIPY-1-CI** in different solvents in the region from 400 nm to 600 nm at 25 °C.

Table 1: Solvent dependent absorption maxima of **SBDIPY-1-CI**.

Solvent	Absorption maximum $\lambda_{\max}^{\text{abs}}$ (nm)
Acetonitrile	497
Benzene	504
o-Dichlorobenzene	505
Dichloromethane	501
Tetrahydrofuran	500

5.3. Analysis of the decomposition process

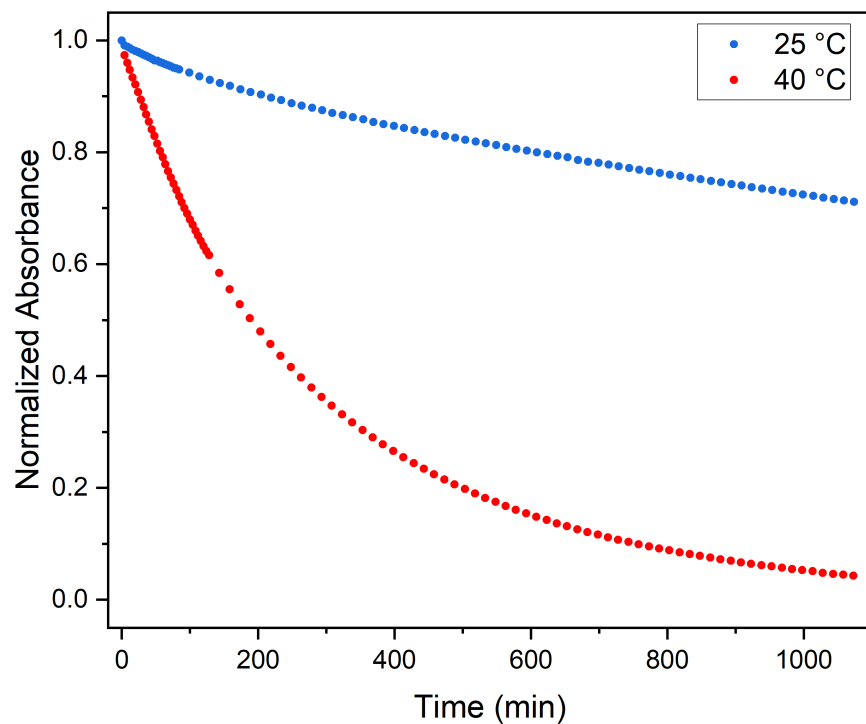


Figure 2: Time course measurement of normalized absorbance of **SBDIPY-1-Cl** major UV band in THF (500 nm) at 25 °C and 40 °C.

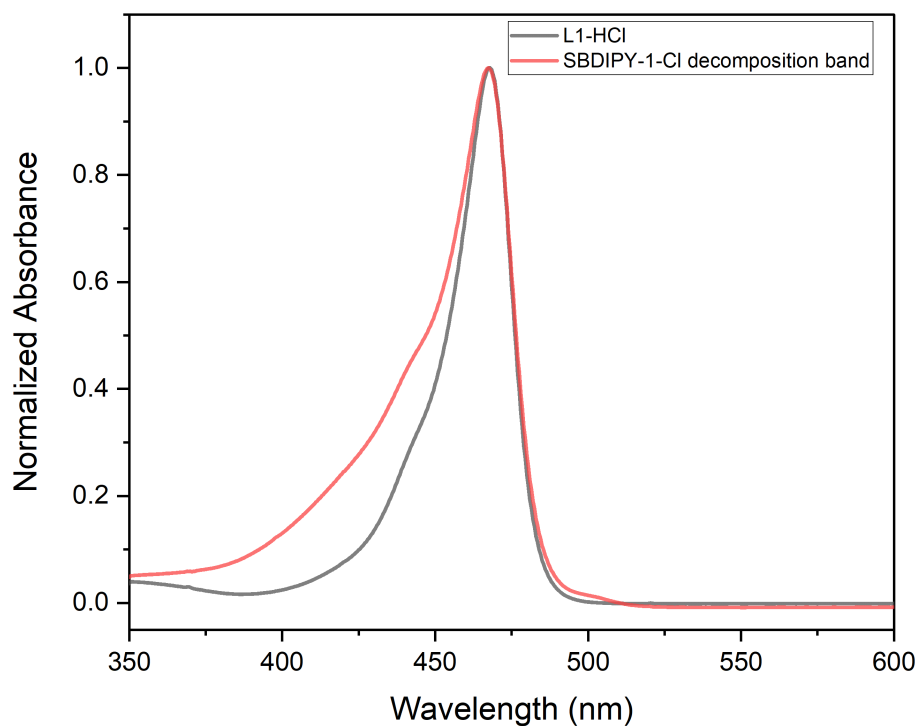


Figure 3: Overlapped normalized absorbance spectra of **L1-HCl** and **SBDIPY-1-Cl** upon full conversion to a single decomposition band ($\lambda_{\text{max}}^{\text{abs}} = 468 \text{ nm}$) in THF.

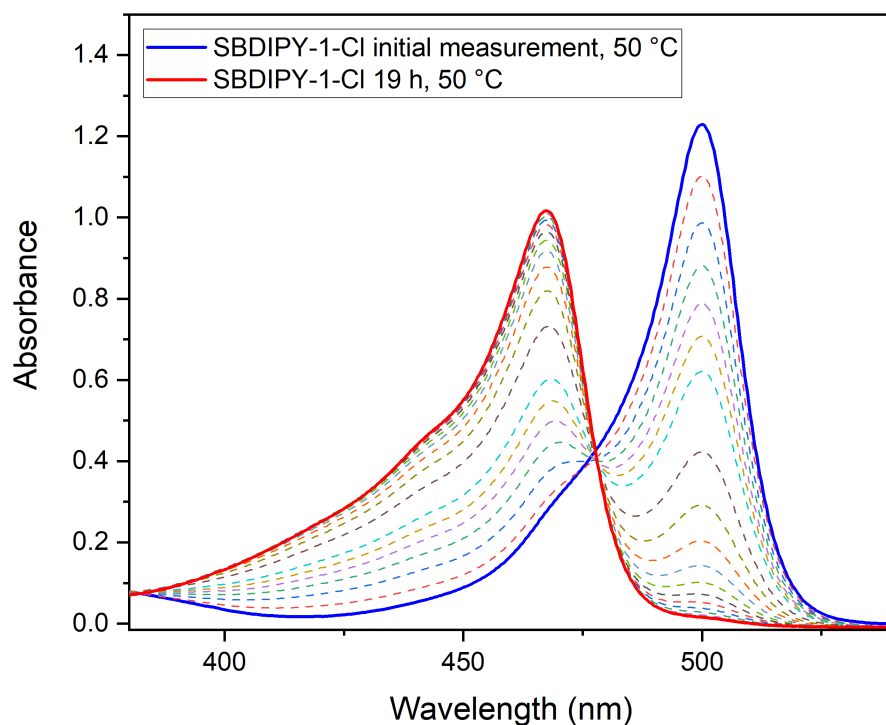


Figure 4: UV/Vis time course measurement of **SBDIPY-1-Cl** in THF ($17 \mu\text{M}$ solution) at $50 \text{ }^\circ\text{C}$. The initial UV/Vis spectrum is highlighted in blue and the spectrum after 19 hours is highlighted in red.

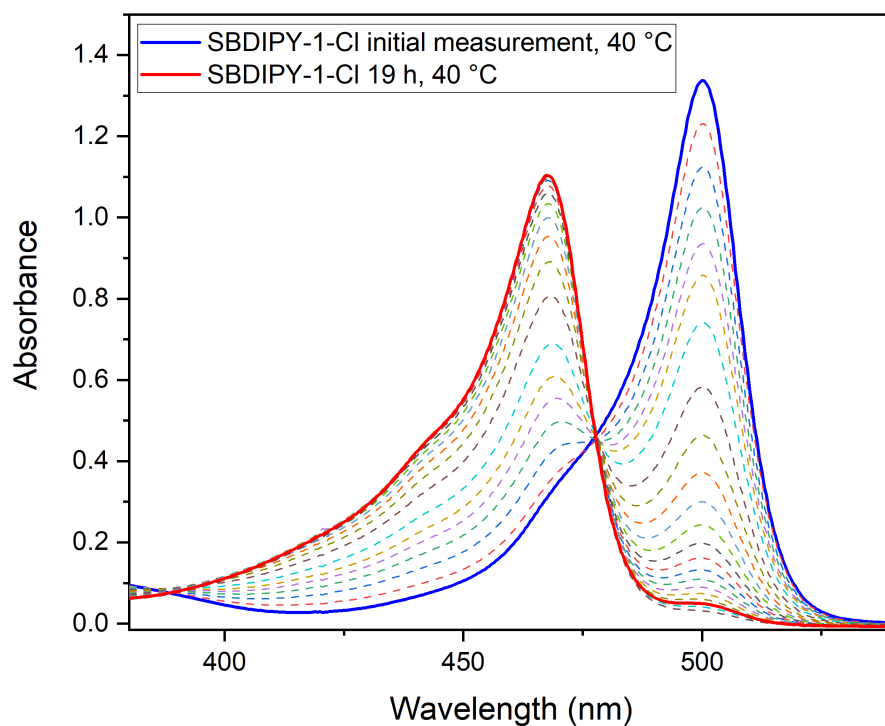


Figure 5: UV/Vis time course measurement of **SBDIPY-1-Cl** in THF (17 μ M solution) at 40 °C. The initial UV/Vis spectrum is highlighted in blue and the spectrum after 19 hours is highlighted in red.

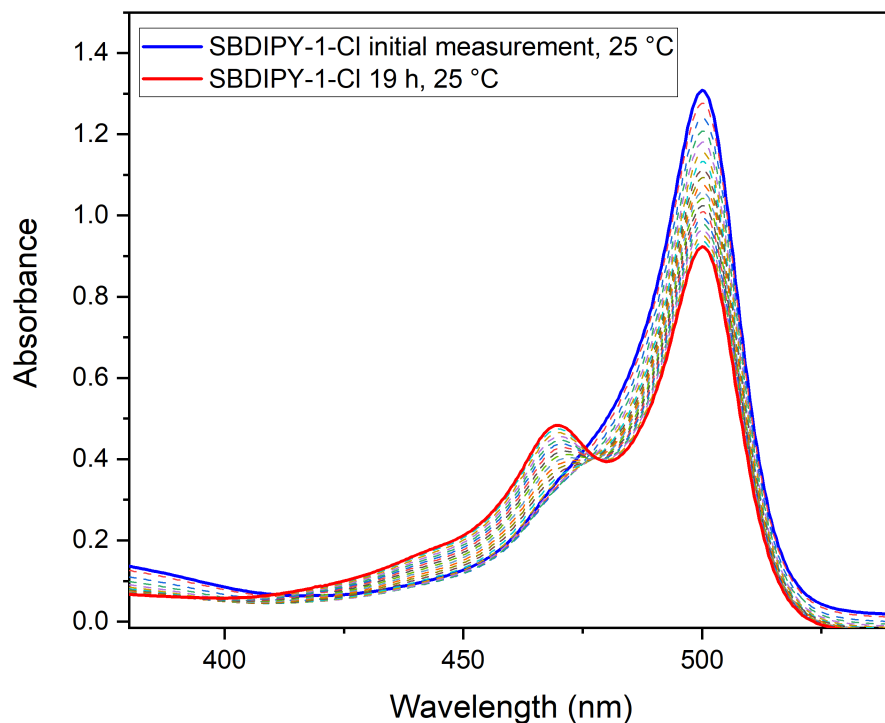


Figure 6: UV/Vis time course measurement of **SBDIPY-1-Cl** in THF (17 μ M solution) at 25 °C. The initial UV/Vis spectrum is highlighted in blue and the spectrum after 19 hours is highlighted in red.

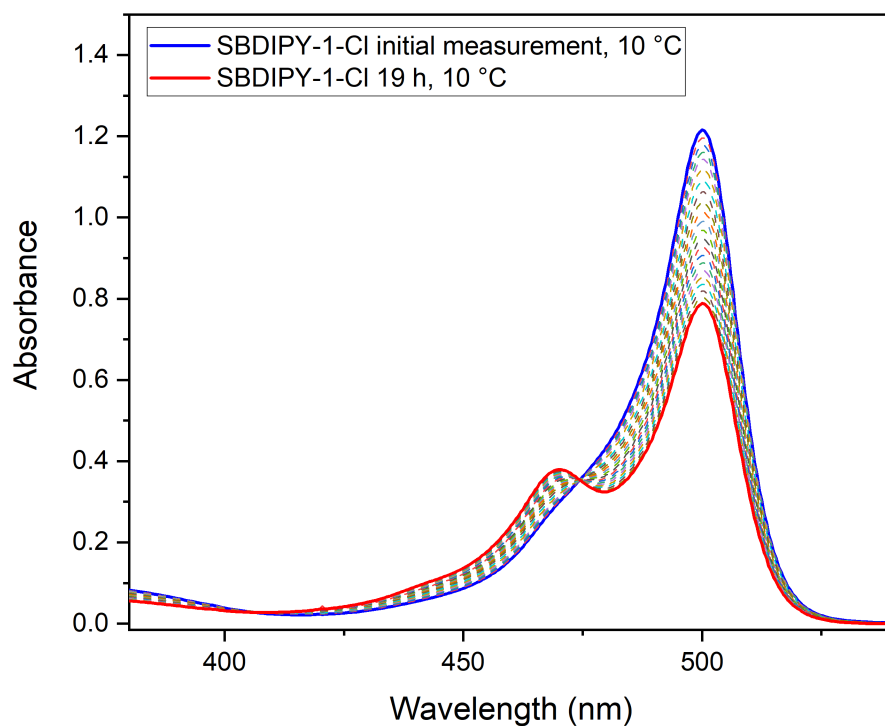


Figure 7: UV/Vis time course measurement of **SBDIPY-1-Cl** in THF (17 μM solution) at 10 $^{\circ}\text{C}$. The initial UV/Vis spectrum is highlighted in blue and the spectrum after 19 hours is highlighted in red.

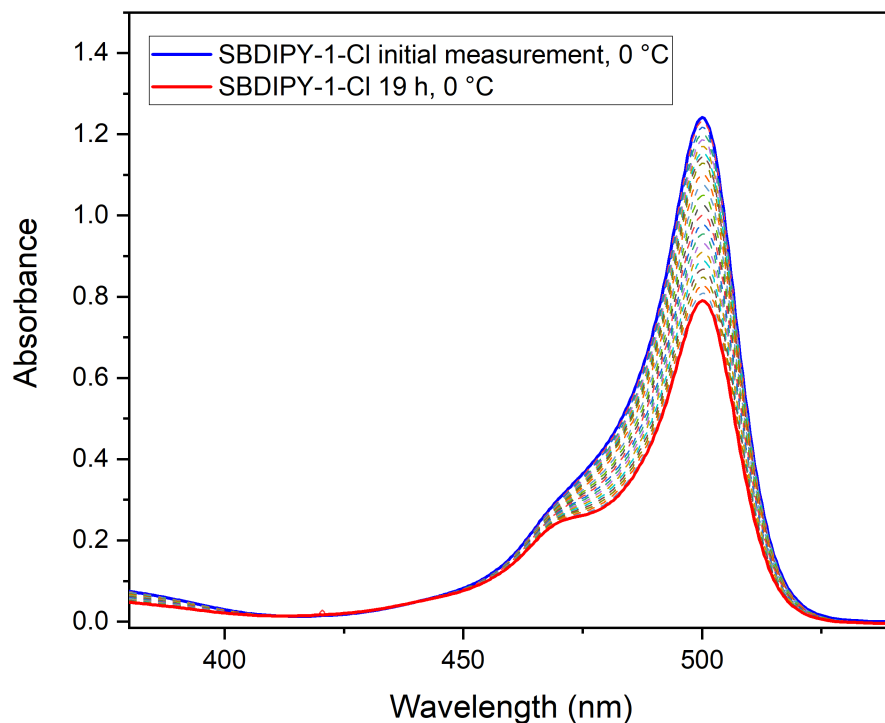


Figure 8: UV/Vis time course measurement of **SBDIPY-1-Cl** in THF (17 μM solution) at 0 $^{\circ}\text{C}$. The initial UV/Vis spectrum is highlighted in blue and the spectrum after 19 hours is highlighted in red.

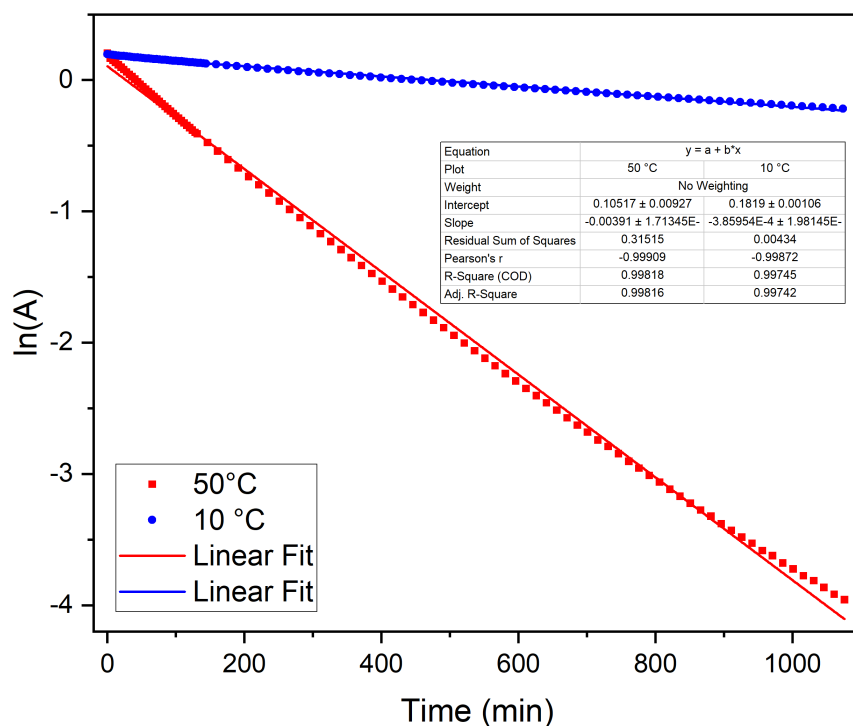


Figure 9: SBDIPY-1-Cl major UV band (500 nm) decay plot of $\ln(A)$ against time at 10 °C (blue) and 50 °C (red) in THF.

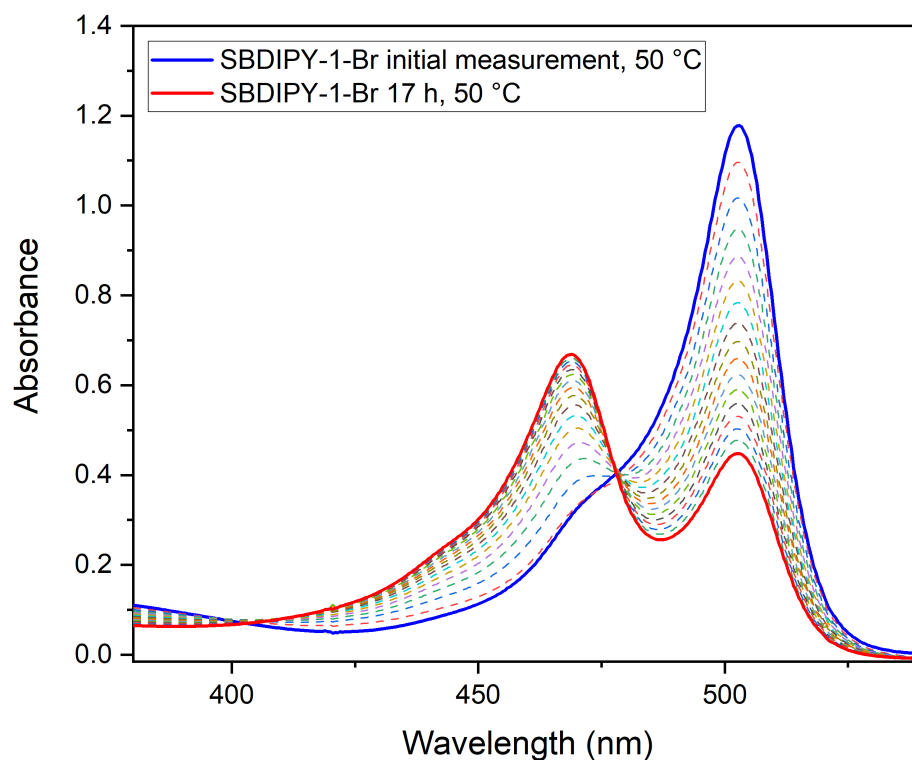


Figure 10: UV/Vis time course measurement of SBDIPY-1-Br in THF (17 μM solution) at 50 °C. The initial UV/Vis spectrum is highlighted in blue and the spectrum after 17 hours is highlighted in red.

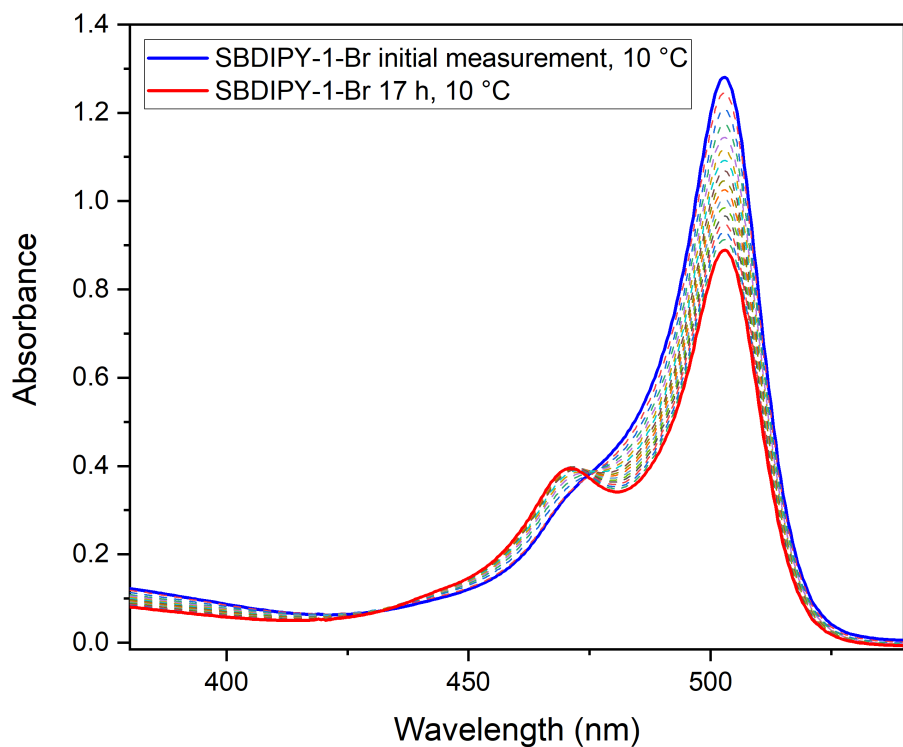


Figure 11: UV/Vis time course measurement of **SBDIPY-1-Br** in THF (17 μM solution) at 10 $^{\circ}\text{C}$. The initial UV/Vis spectrum is highlighted in blue and the spectrum after 17 hours is highlighted in red.

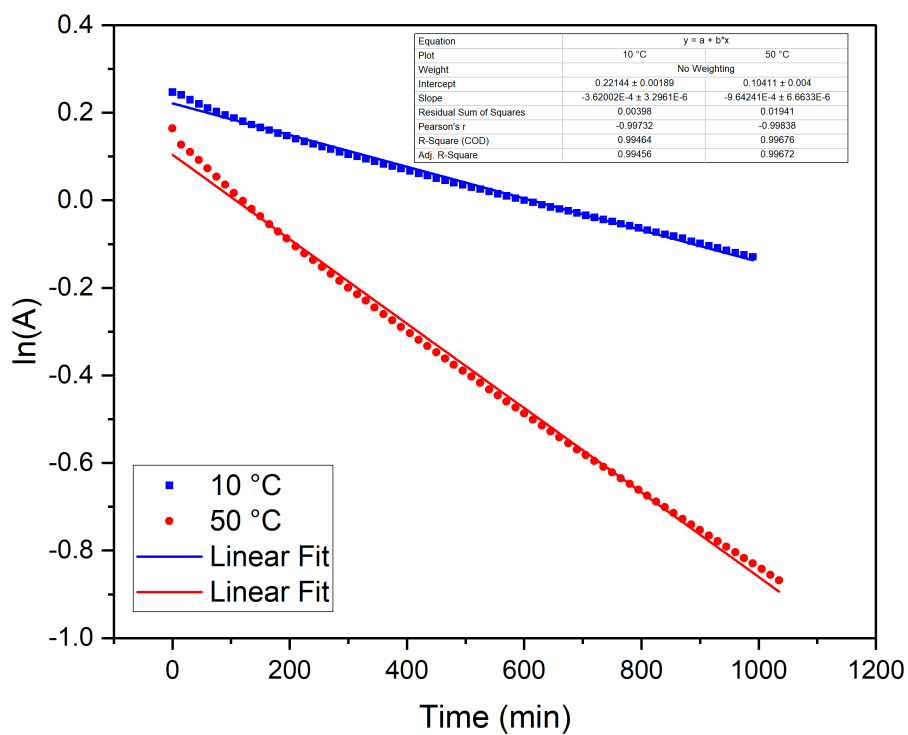


Figure 12: **SBDIPY-1-Br** major UV band (503 nm) decay plot of $\ln(A)$ against time at 10 $^{\circ}\text{C}$ (blue) and 50 $^{\circ}\text{C}$ (red) in THF.

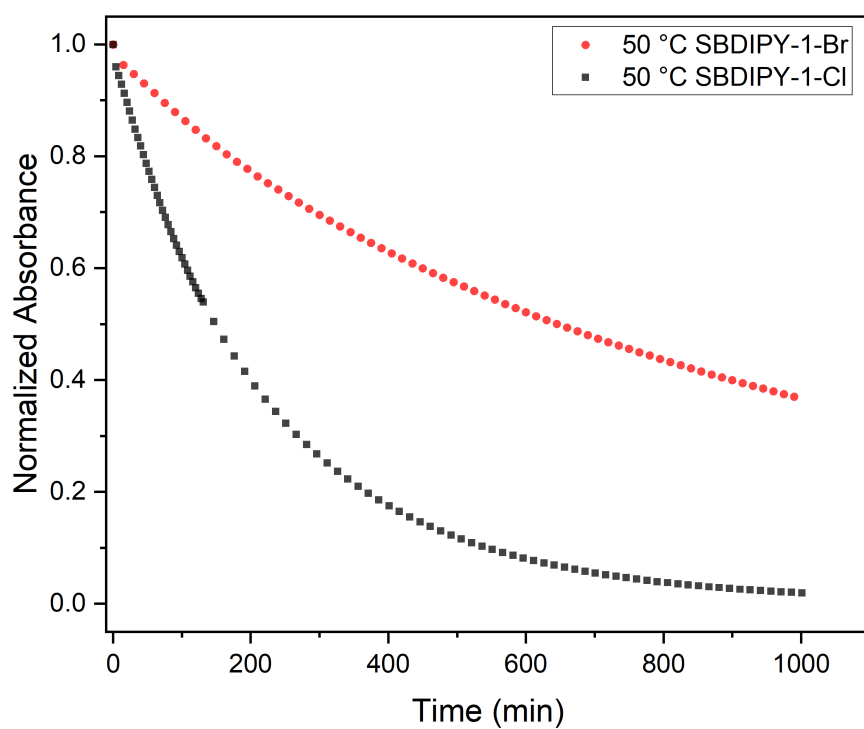


Figure 13: Time resolved absorbance decay of major UV band of **SBDIPY-1-Cl** (500 nm) and **SBDIPY-1-Br** (503 nm) in THF at 50 °C.

5.4. Determination of molar absorption coefficients (ϵ)

Molar absorption coefficients ϵ were obtained by plotting the absorbance A against sample concentration c as the slope k of the linear regression analysis as in:

$$A = k \cdot c + b$$

where b denotes the y -axis intercept. An overview of calculated ϵ -values is given in Table 2.

Table 2: Calculated molar absorption coefficients.

Complex	ϵ ($M^{-1} \cdot cm^{-1}$)
SBDIPY-1-Cl	75460
SBDIPY-1 ⁺ -Cl	52960
SBDIPY-1-Br	67640
SBDIPY-2-Cl	71660
SBDIPY-3-Cl	75280

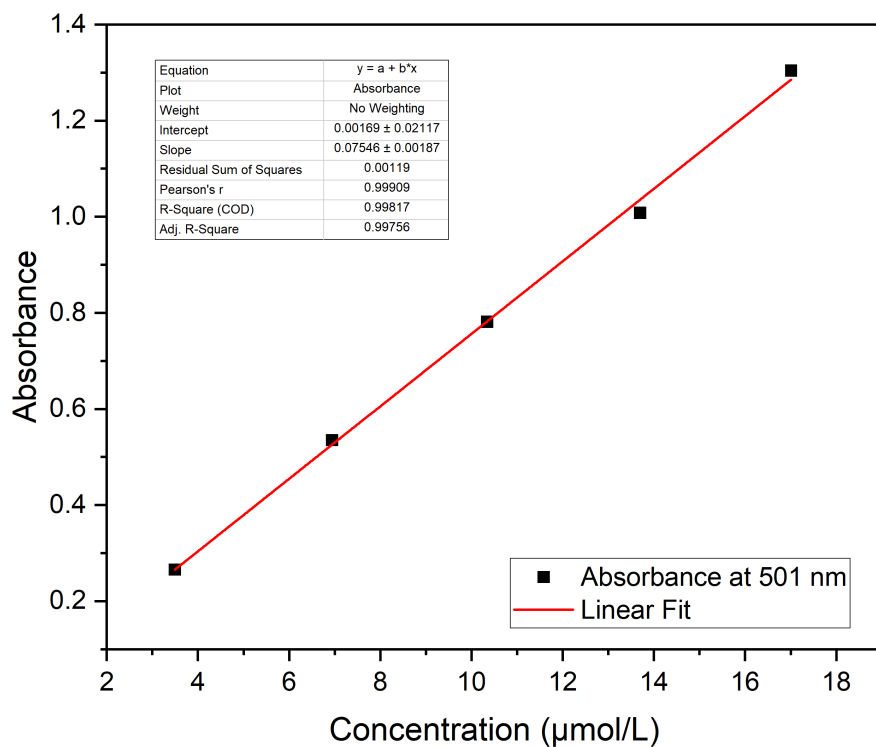


Figure 14: Absorbance of **SBDIPY-1-Cl** in CH_2Cl_2 (501 nm) plotted against respective sample concentration.

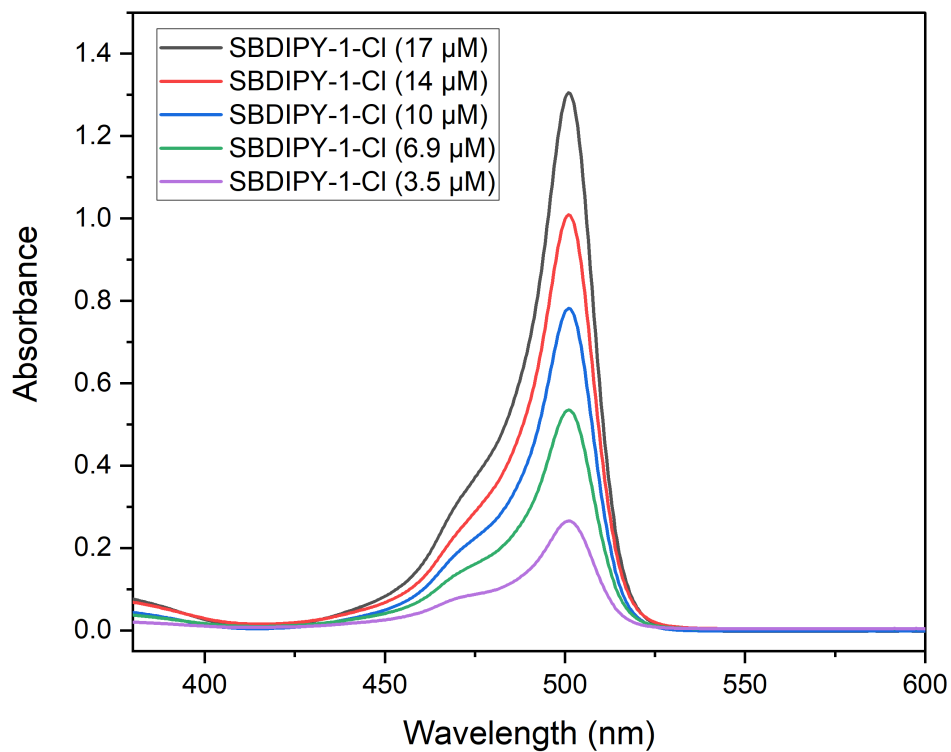


Figure 15: UV/Vis spectra of dilution series of **SBDIPY-1-Cl** in CH_2Cl_2 at 5 °C.

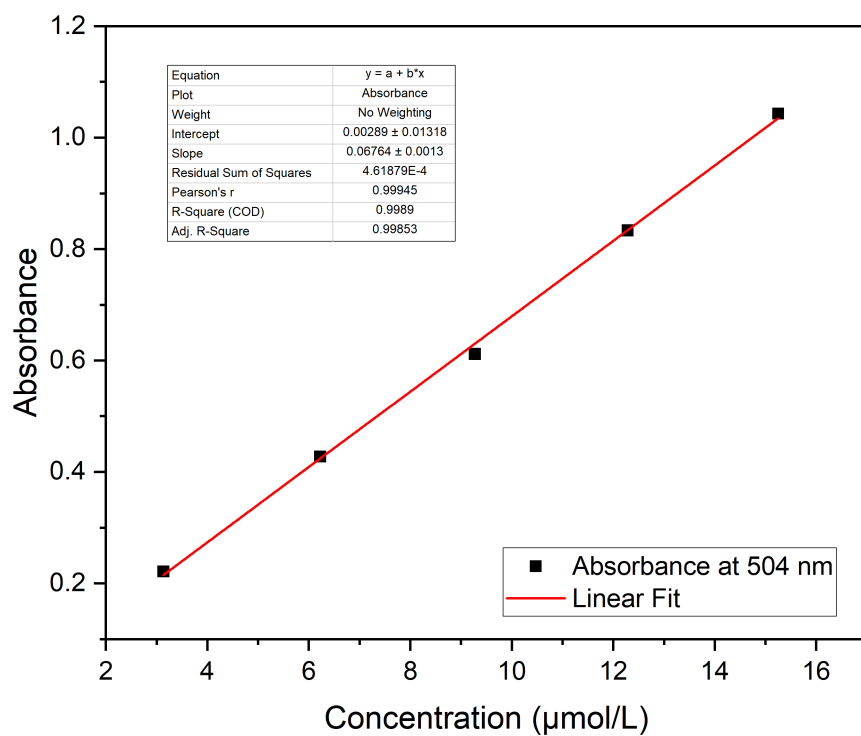


Figure 16: Absorbance of **SBDIPY-1-Br** in CH_2Cl_2 (504 nm) plotted against respective sample concentration.

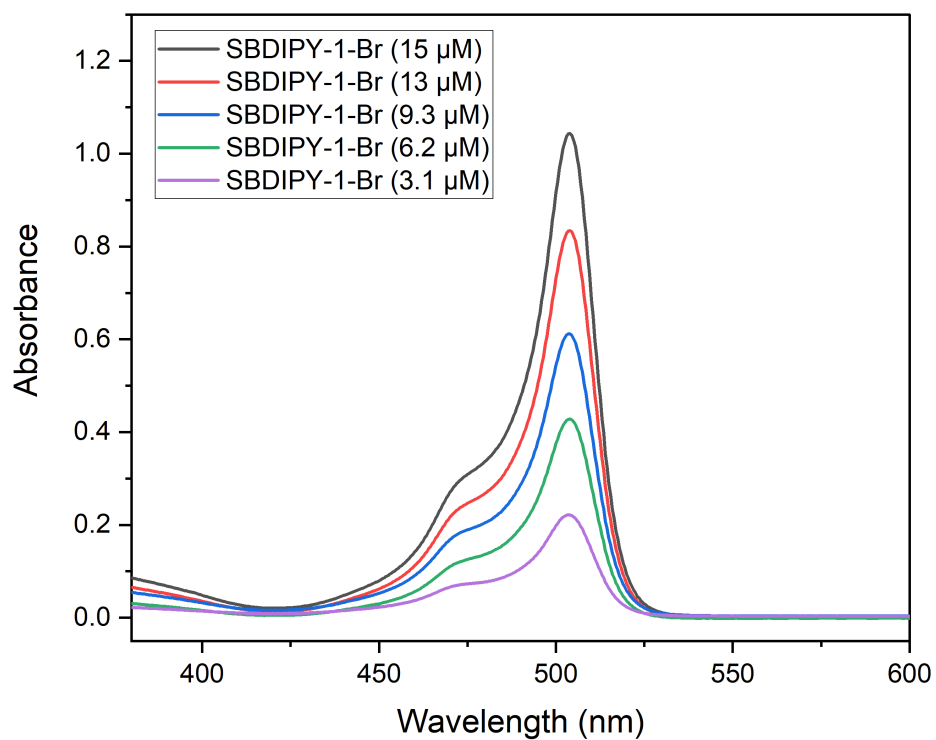


Figure 17: UV/Vis spectra of dilution series of **SBDIPY-1-Br** in CH_2Cl_2 at 5 °C.

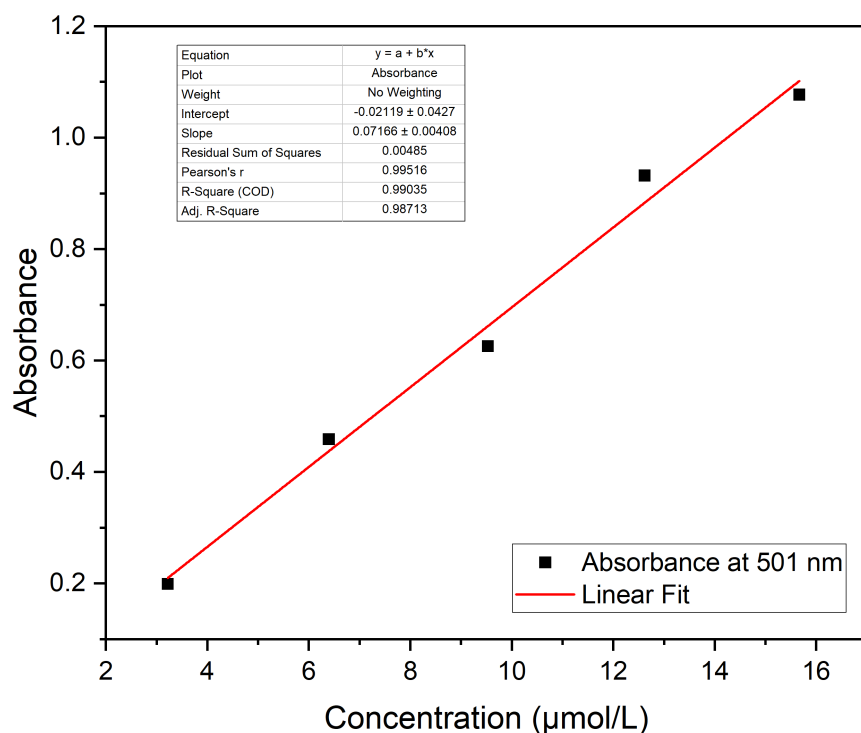


Figure 18: Absorbance of **SBDIPY-2-Cl** in CH₂Cl₂ (501 nm) plotted against respective sample concentration.

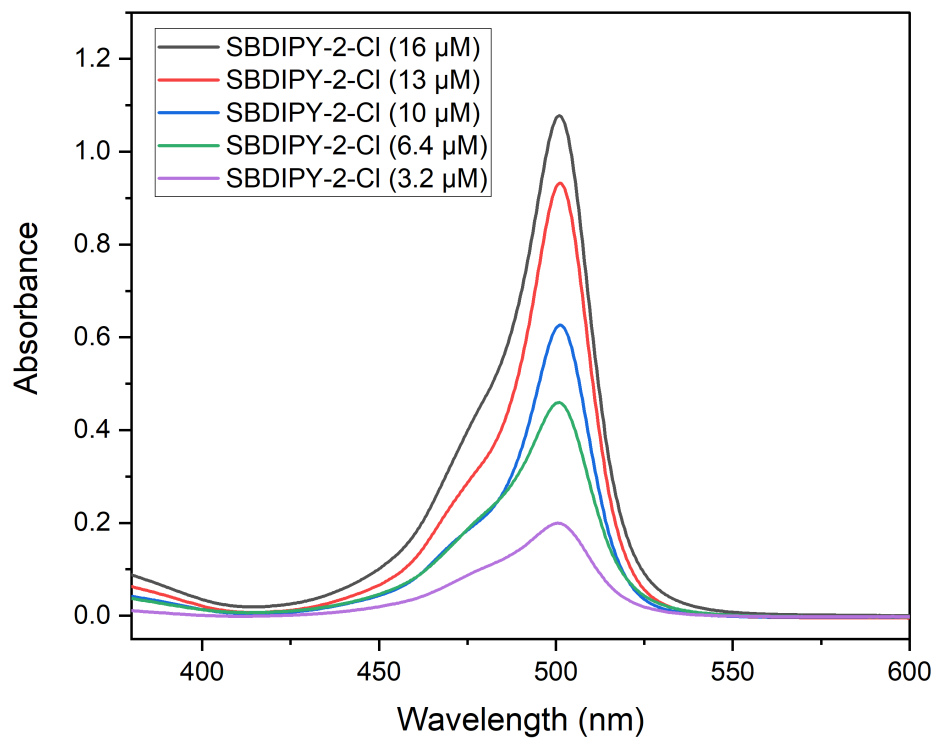


Figure 19: UV/Vis spectra of dilution series of **SBDIPY-2-Cl** in CH₂Cl₂ at 5 °C.

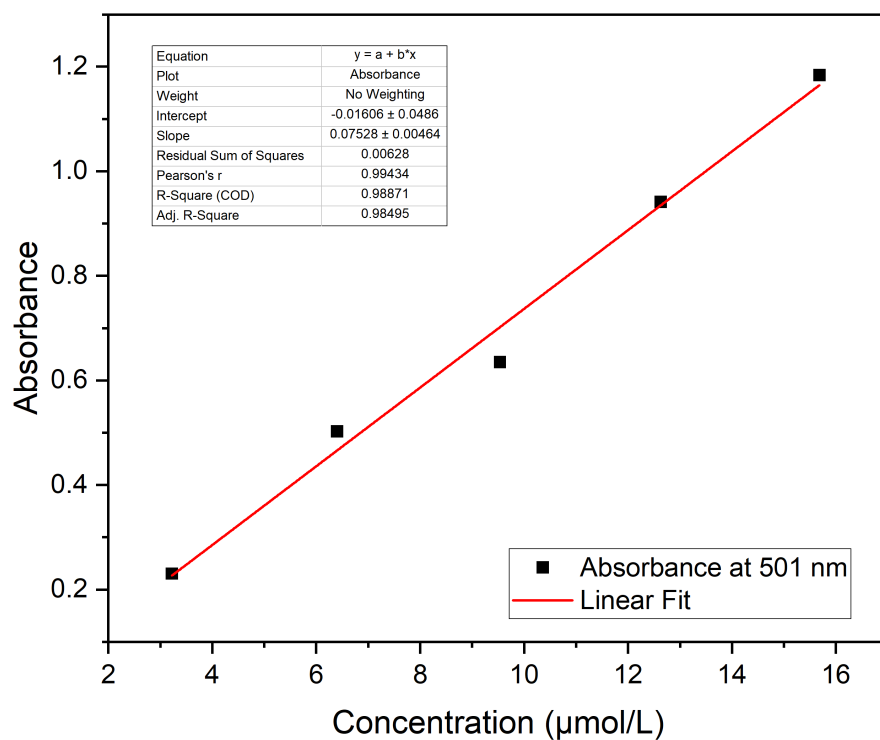


Figure 20: Absorbance of **SBDIPY-3-Cl** in CH_2Cl_2 (501 nm) plotted against respective sample concentration.

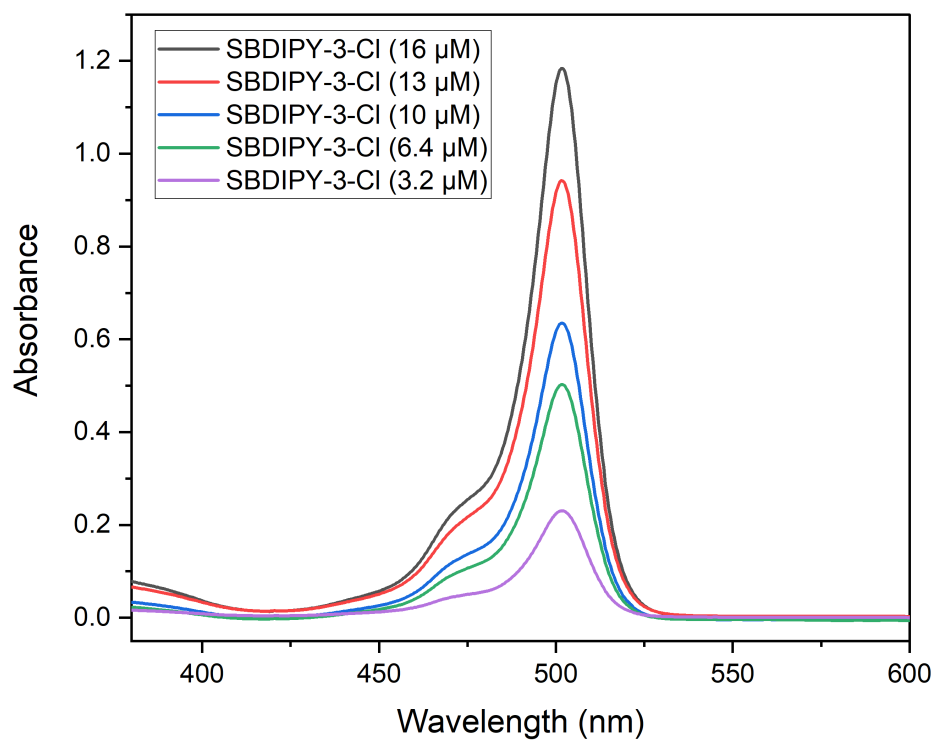


Figure 21: UV/Vis spectra of dilution series of **SBDIPY-3-Cl** in CH_2Cl_2 at 5 °C.

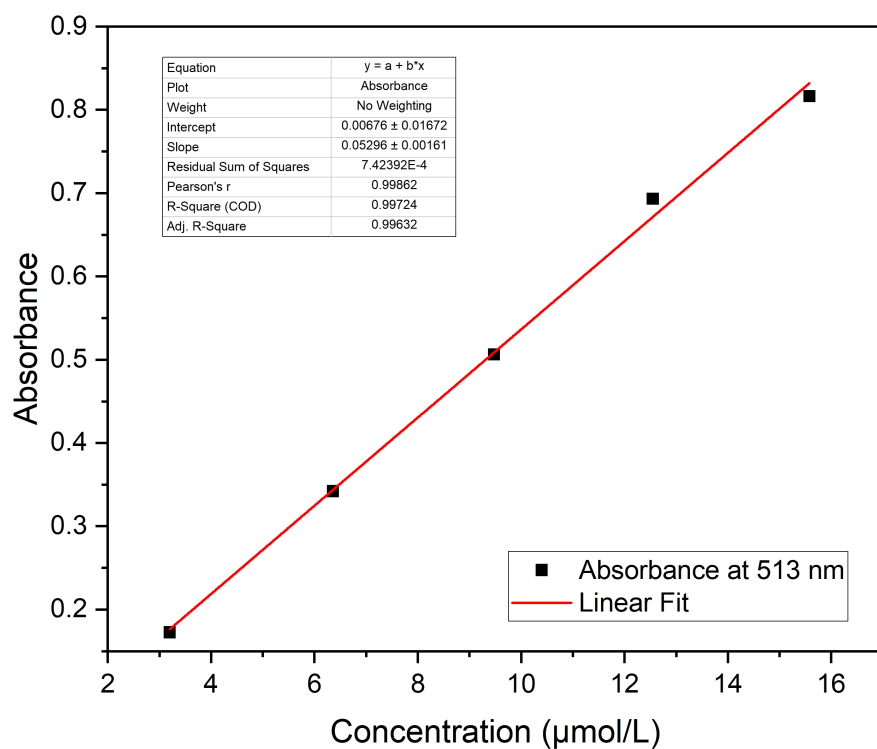


Figure 22: Absorbance of **SBDIPY-1⁺-Cl** in CH₂Cl₂ (513 nm) plotted against respective sample concentration.

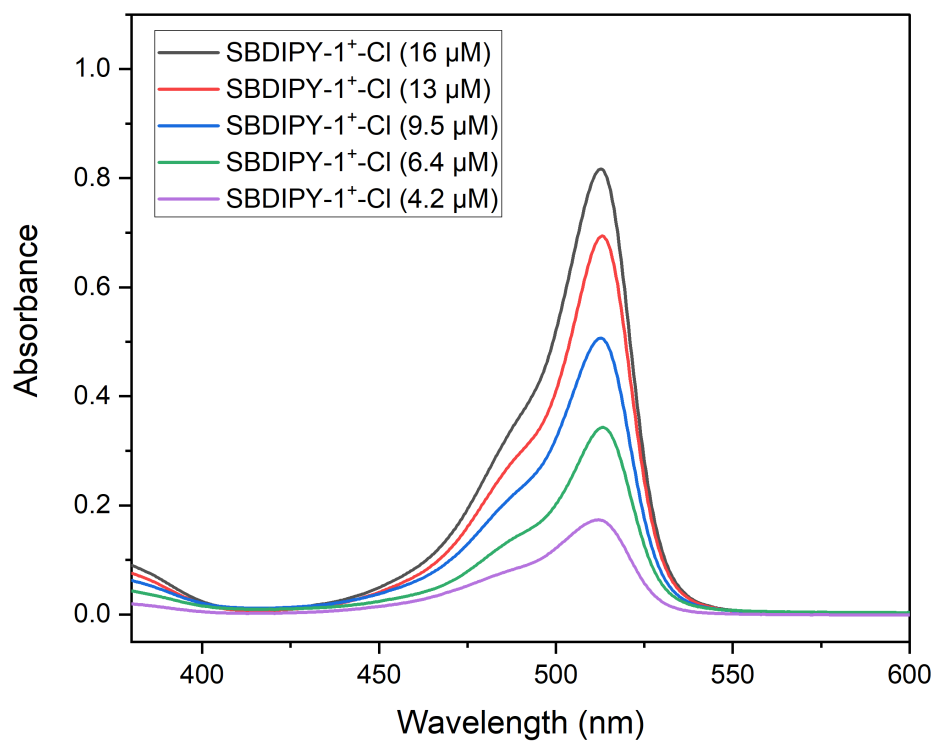


Figure 23: UV/Vis spectra of dilution series of **SBDIPY-1⁺-Cl** in CH₂Cl₂ at 5 °C.

5.5. UV/Vis spectroscopy of SBDIPY-1-F

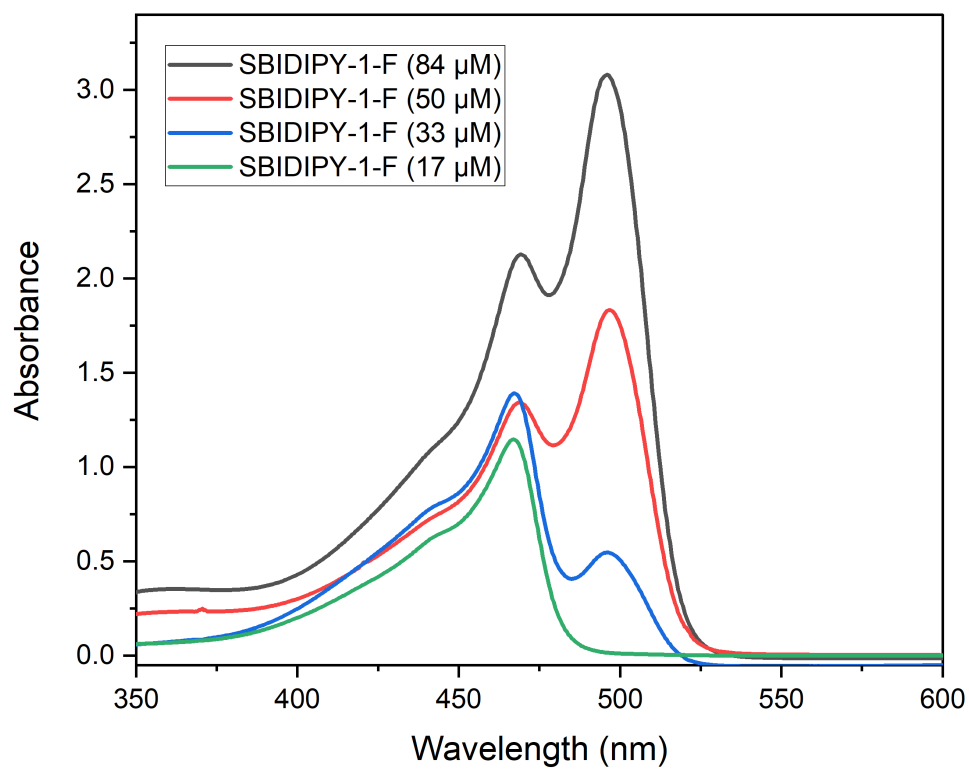


Figure 24: UV/Vis spectra of **SBDIPY-1-F** at different sample concentrations in CH₂Cl₂ at -10 °C.

5.6. UV/Vis spectroscopy of BIDIPY complexes

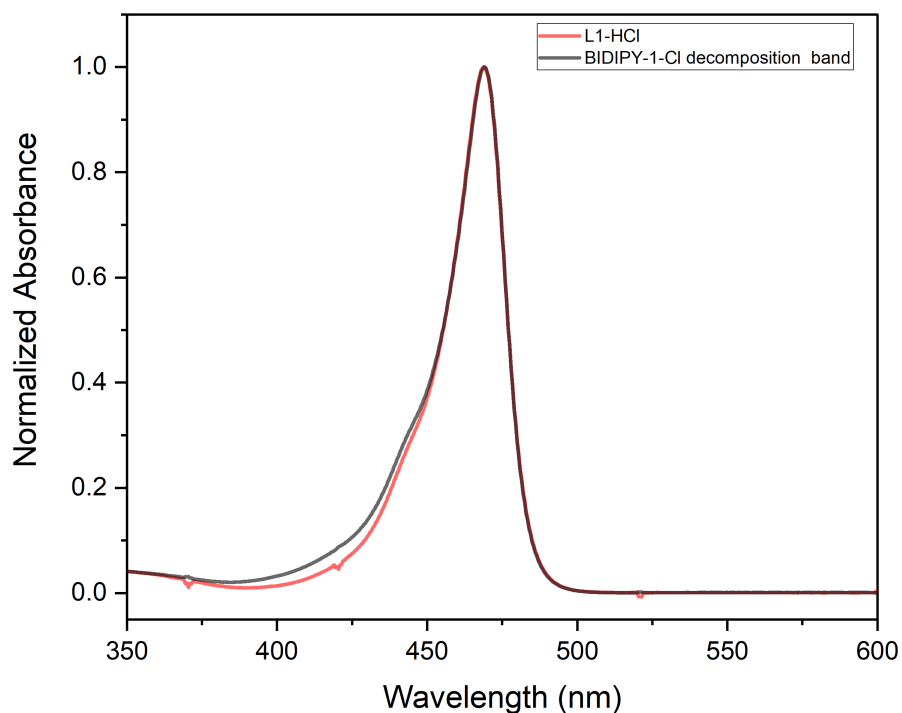


Figure 25: Overlapped normalized absorbance spectra of **L1-HCl** and **BIDIPY-1-Cl** upon full conversion to a single decomposition band ($\lambda_{\text{max}}^{\text{abs}} = 469 \text{ nm}$) in CH_2Cl_2 .

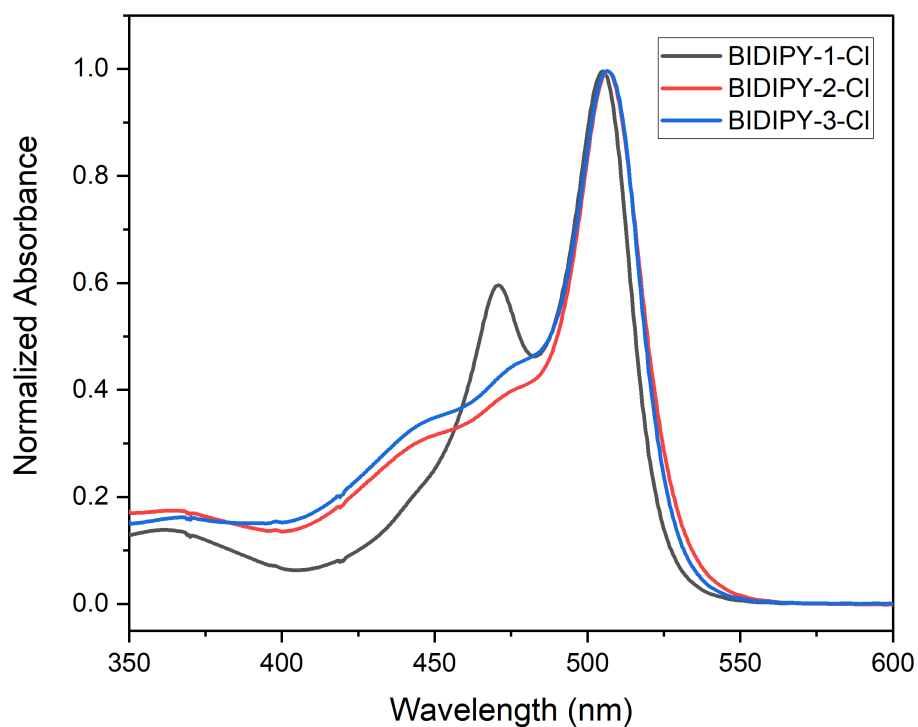


Figure 26: Normalized UV/Vis spectra of **BIDIPY** complexes in CH_2Cl_2 at $5 \text{ }^\circ\text{C}$.

5.7. Fluorescence spectroscopy

Relative quantum yields φ_{rel} of **SBDIPY** probes were obtained at 5 °C using **BODIPY-F** ($\varphi_{\text{ref}} = 0.95$) as a reference.^[8] The quantum yields were determined by plotting the integrated fluorescence emission between 490 and 585 nm against the absorbance of five differently-concentrated solutions of test compounds in CH_2Cl_2 with absorbance values ranging from 0.02 to 0.09. Respective quantum yields φ_{rel} (see Fig. 27) were calculated using the following equation:

$$\varphi_{\text{rel}} = \varphi_{\text{ref}} \frac{m}{m_{\text{ref}}} \cdot \left(\frac{n}{n_{\text{ref}}} \right)^2$$

where m is the slope of **SBDIPY** probes, m_{ref} the slope of the BODIPY reference sample and n the refractive index of the solvent (CH_2Cl_2).

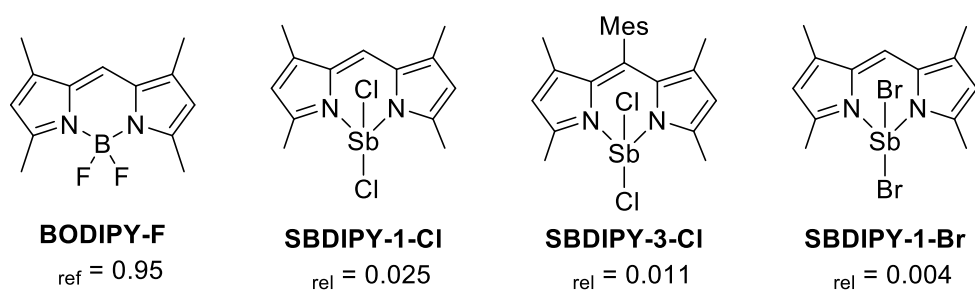


Figure 27: Overview of quantum yields in CH_2Cl_2 . Quantum yield of the reference **BODIPY-F** was taken from literature.^[8]

Table 3: Overview of maximum absorption and emission values, Stokes shifts and quantum yields (relative to **BODIPY-F**) of the respective **SBDIPY** complexes.^[8]

Complex	Absorption maximum $\lambda_{\text{max}}^{\text{abs}}$ (nm)	Emission maximum $\lambda_{\text{max}}^{\text{em}}$ (nm)	Stokes shift (cm^{-1})	Quantum Yield $\phi_{\text{rel}}^{\text{[8]}}$
SBDIPY-1-Cl	501	516	580	0.025
SBDIPY-1-Br	504	518	536	0.004
SBDIPY-1-F	496	522	1004	n.a.
SBDIPY-2-Cl	501	520	729	n.a.
SBDIPY-3-Cl	501	523	840	0.011
SBDIPY-1⁺-Cl	513	518	188	n.a.

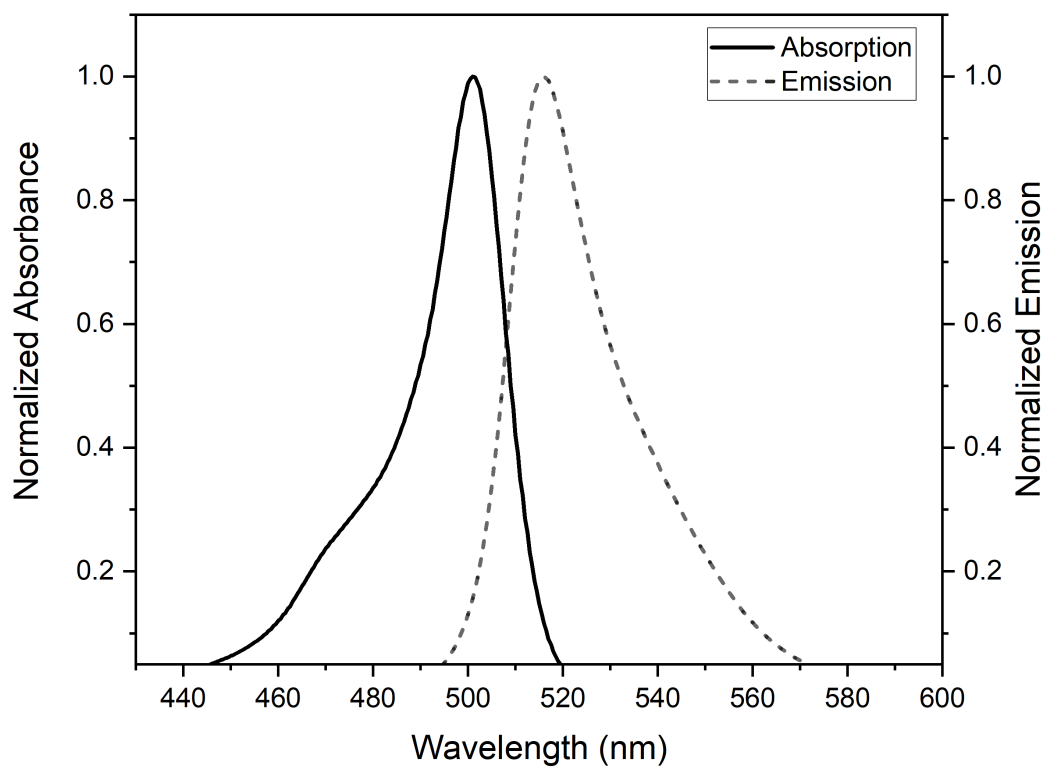


Figure 28: Normalized absorbance and fluorescence emission spectra of **SBDIPY-1-Cl** in CH_2Cl_2 . Emission was recorded at an excitation wavelength of 460 nm.

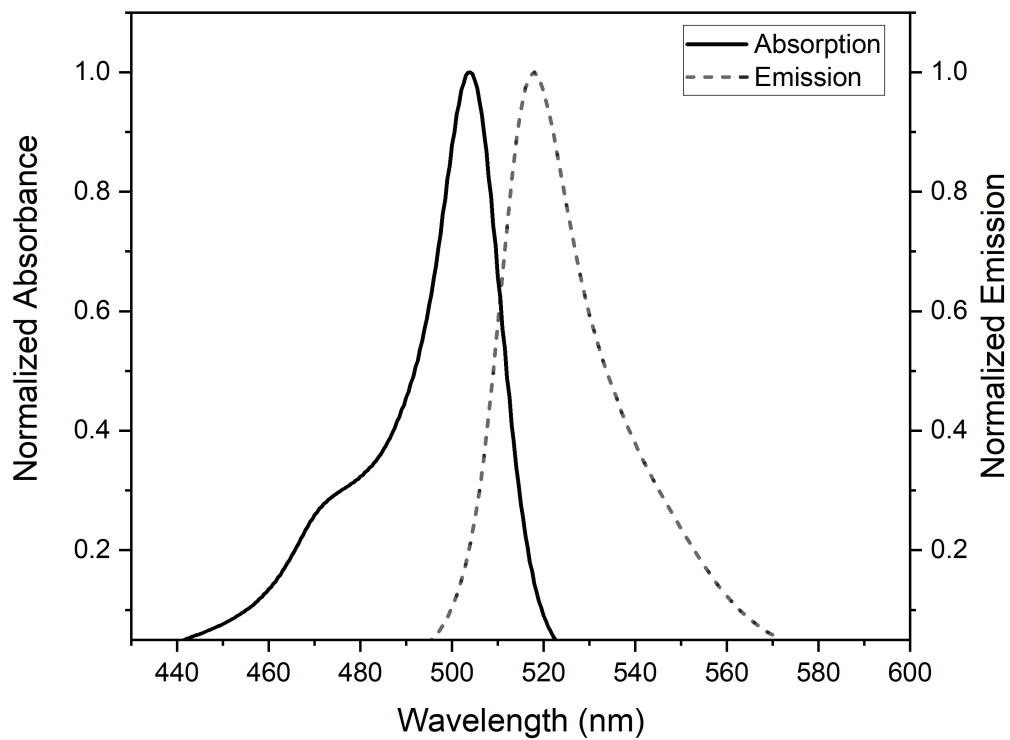


Figure 29: Normalized absorbance and fluorescence emission spectra of **SBDIPY-1-Br** in CH_2Cl_2 . Emission was recorded at an excitation wavelength of 460 nm.

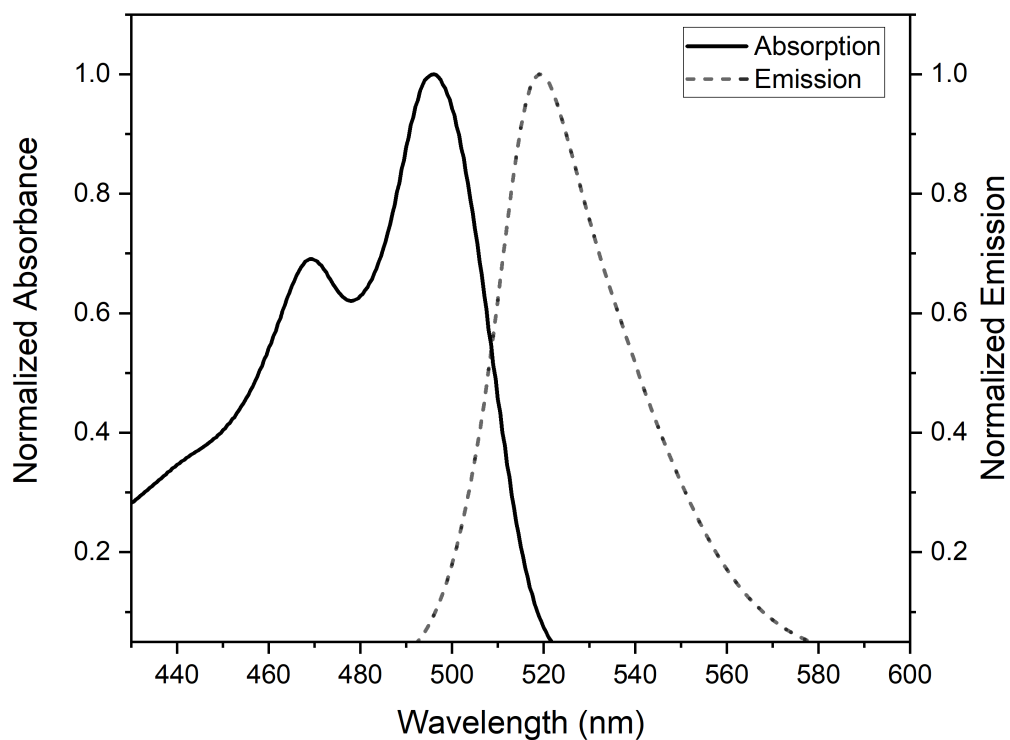


Figure 30: Normalized absorbance and fluorescence emission spectra of **SBDIPY-1-F** in CH₂Cl₂. Emission was recorded at an excitation wavelength of 460 nm.

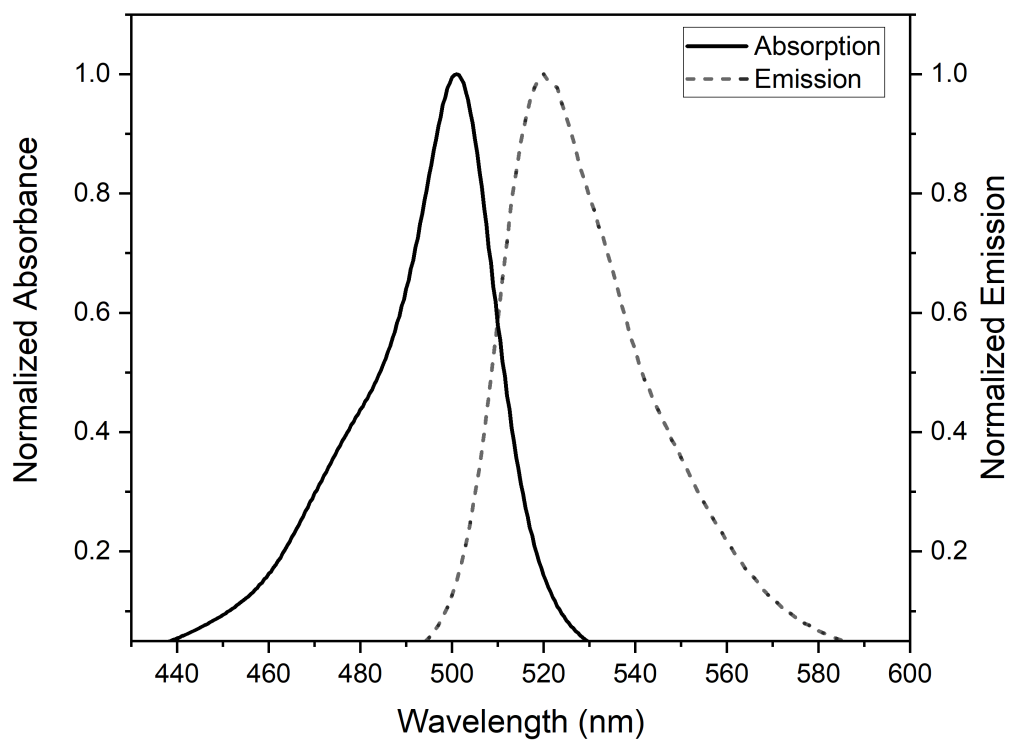


Figure 31: Normalized absorbance and fluorescence emission spectra of **SBDIPY-2-Cl** in CH₂Cl₂. Emission was recorded at an excitation wavelength of 460 nm.

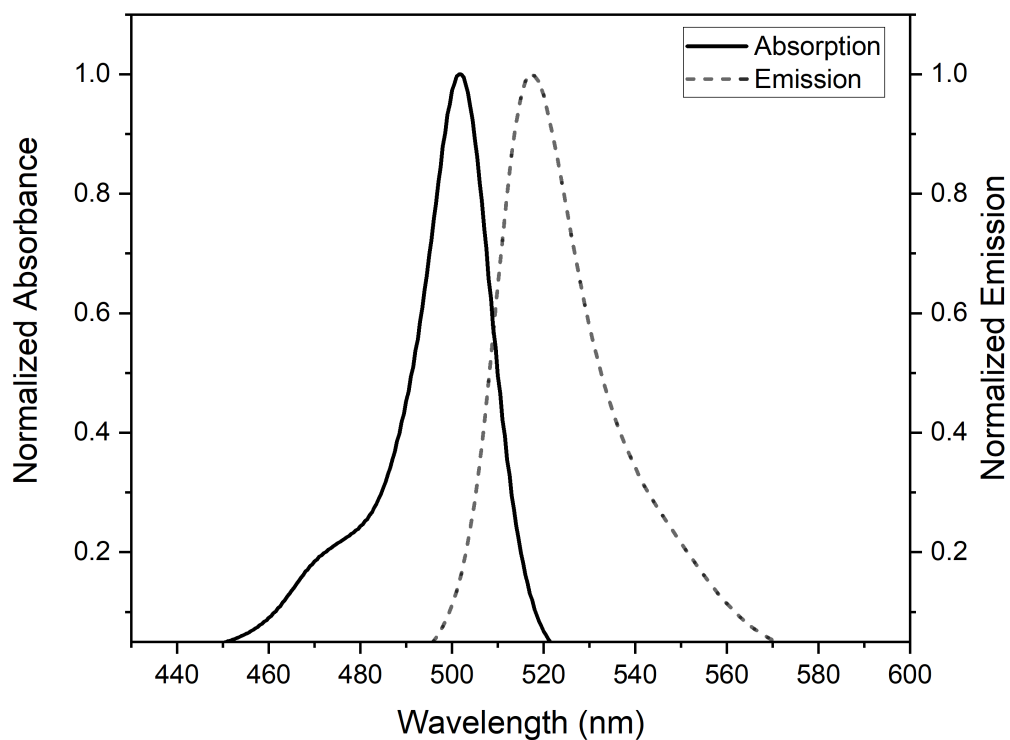


Figure 32: Normalized absorbance and fluorescence emission spectra of **SBDIPY-3-Cl** in CH₂Cl₂. Emission was recorded at an excitation wavelength of 460 nm.

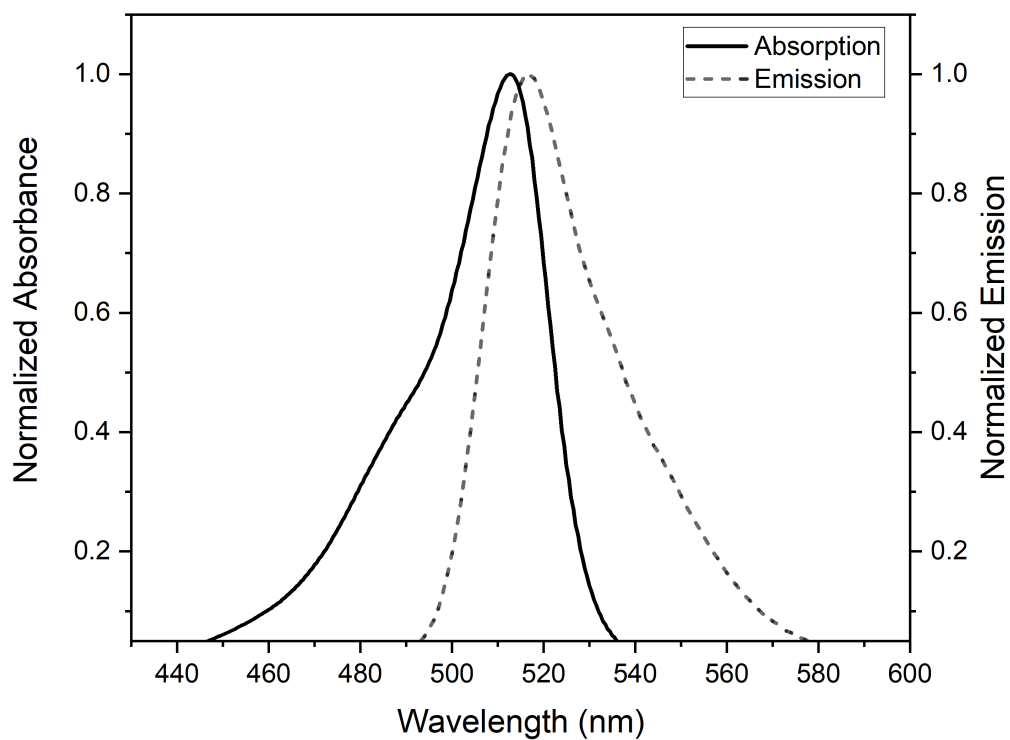


Figure 33: Normalized absorbance and fluorescence emission spectra of **SBDIPY-1⁺-Cl** in CH₂Cl₂. Emission was recorded at an excitation wavelength of 460 nm.

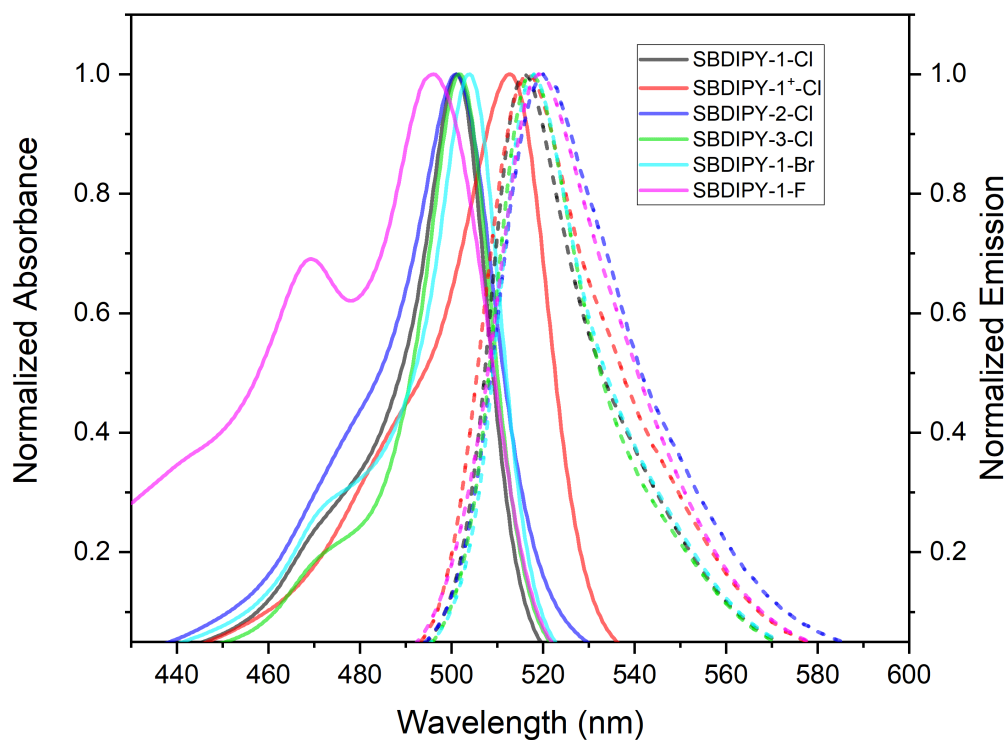


Figure 34: Overview of normalized absorbance and fluorescence emission spectra of **SBDIPY** complexes in CH_2Cl_2 . Emission was recorded at an excitation wavelength of 460 nm.

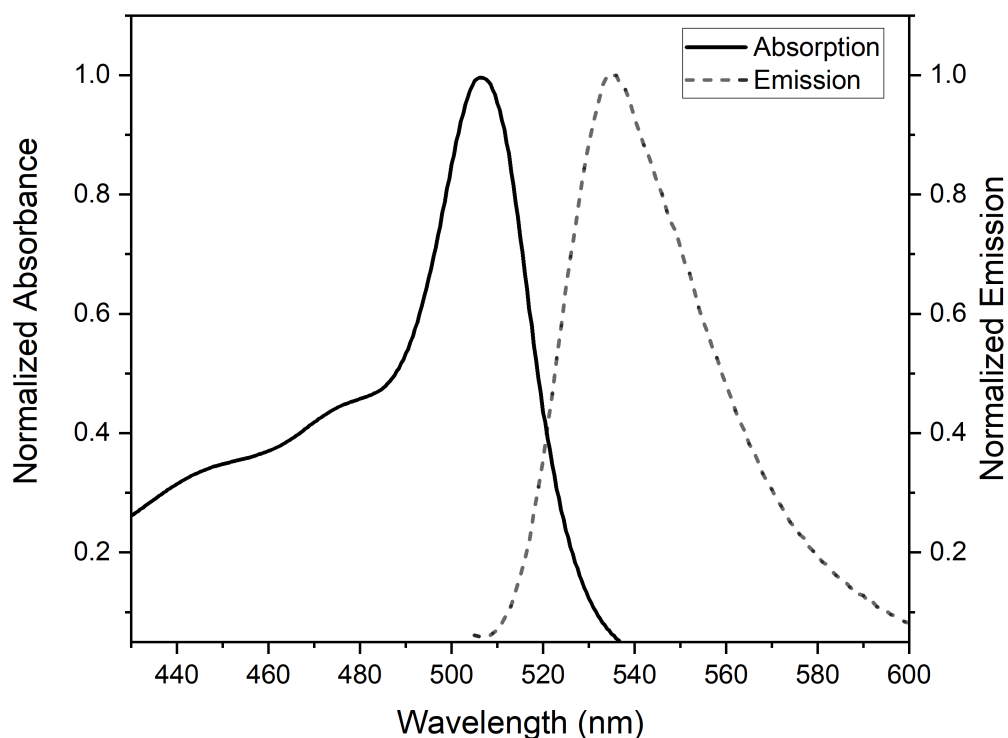


Figure 35: Normalized absorbance and fluorescence emission spectra of **BIDIPY-3-Cl** in CH_2Cl_2 . Emission was recorded at an excitation wavelength of 460 nm. Maximum absorption recorded at $\lambda_{\text{max}}^{\text{abs}} = 506 \text{ nm}$ and maximum emission recorded at $\lambda_{\text{max}}^{\text{em}} = 535 \text{ nm}$.

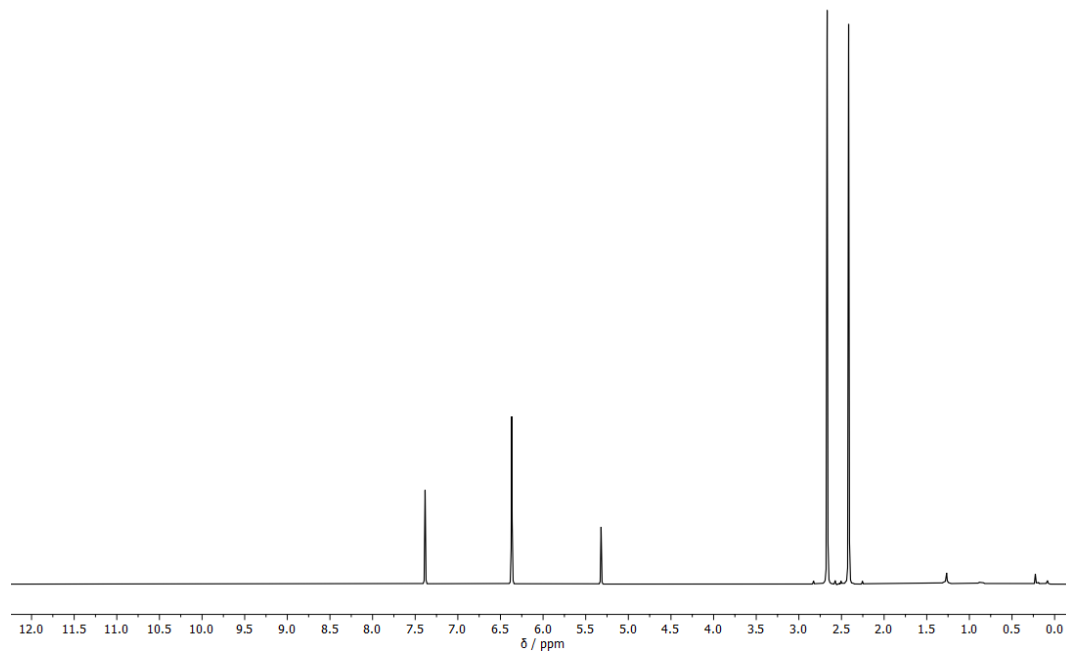
6. Theoretical Analysis

Computational analysis was employed to optimize the structures of differently substituted dipyrin derivatives, to compare the effect of the substituents on the electronic characteristics of the fluorophores. All the geometries were optimized at the r²SCAN-3c level of theory^[9], using CH₂Cl₂ or toluene in the implicit CPCM solvent method as implemented in the ORCA 5.0.3 software.^[10] The nature of the stationary point was confirmed by means the absence frequency calculations. The electronic transition of all stationary points was refined at the SCS-CIS(D)/def2-TZVPP level using CH₂Cl₂ in the implicit CPCM solvent method.^[11,12] The SCS-CIS(D) scaling parameters used are the following: CTss=0.333, CTos=1.2, Cuss=0.43, CUos=1.24. The ECP used was the def2-ECP automatically called by ORCA for heavier elements. The cartesian coordinates of the optimized geometries can be found on figshare using the following DOI: 10.6084/m9.figshare.22083563

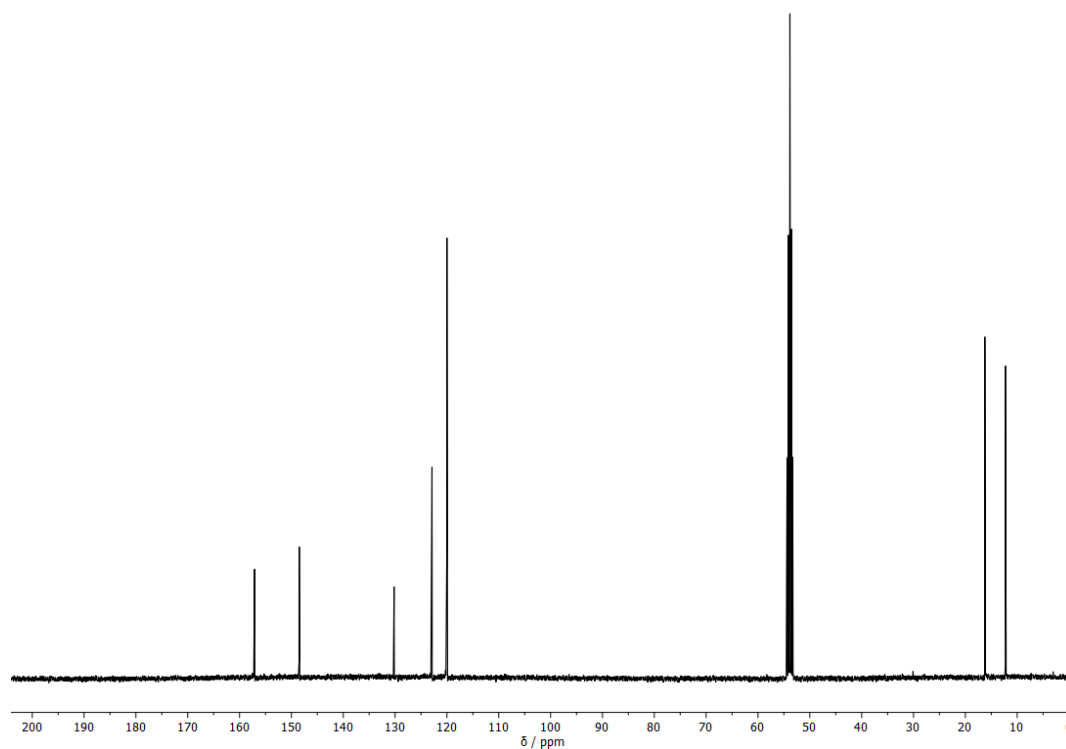
Table 4: Predicted electronic transition of different derivatives at the CPCM-SCS-CIS(D)/def2-TZVPP//CPCM-r²SCAN-3c level.

	Predicted transition	Oscillator strength	HOMO	LUMO
	nm	f	(A.U)	(A.U.)
SBDIPY-1-F	533.6	0.6919	-0.26951	0.01708
SBDIPY-1-Cl	538.8	0.6490	-0.27545	0.01035
SBDIPY-1-Br	542.1	0.6237	-0.27702	0.00816
SBDIPY-2-Cl	546.4	0.5967	-0.27870	0.01155
SBDIPY-3-Cl	553.6	0.5692	-0.27741	0.01240
SBDIPY-1⁺-Cl	553.6	0.6036	-0.29632	-0.01247
BIDIPY-1-Cl	536.8	0.6708	-0.27148	0.01393
BIDIPY-2-Cl	546.0	0.6111	-0.27494	0.01505
BIDIPY-3-Cl	553.9	0.5820	-0.27360	0.01580
BODIPY-F	547.4	0.7099	-0.26369	0.01801
GADIPY	532.0	0.7900	-0.26642	0.01823
PHODIPY	547.1	0.5913	-0.29856	-0.01011

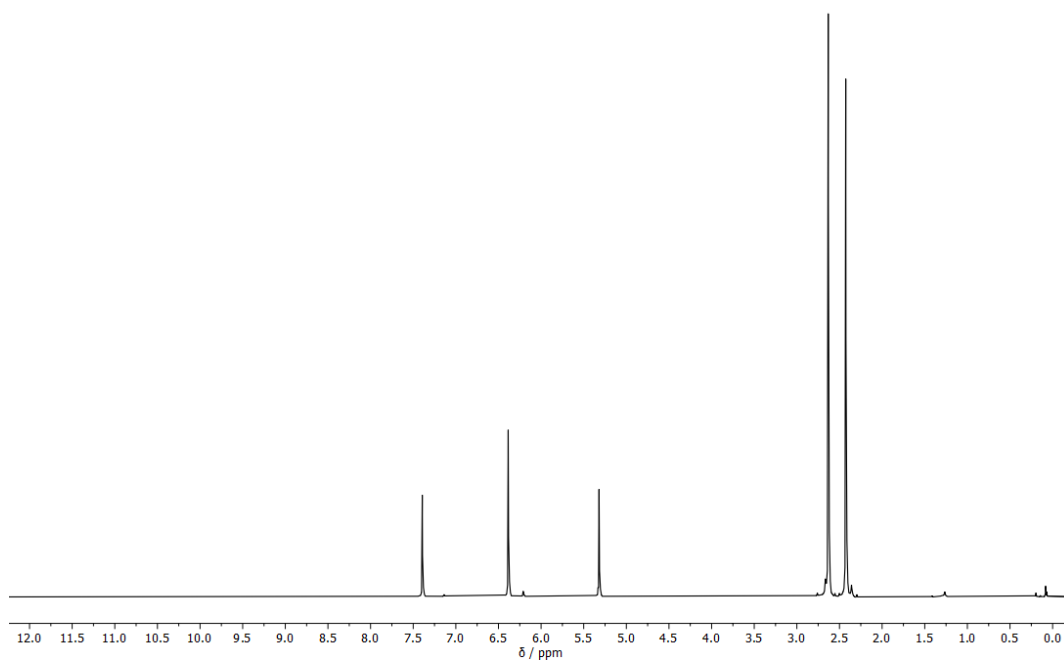
7. NMR spectra



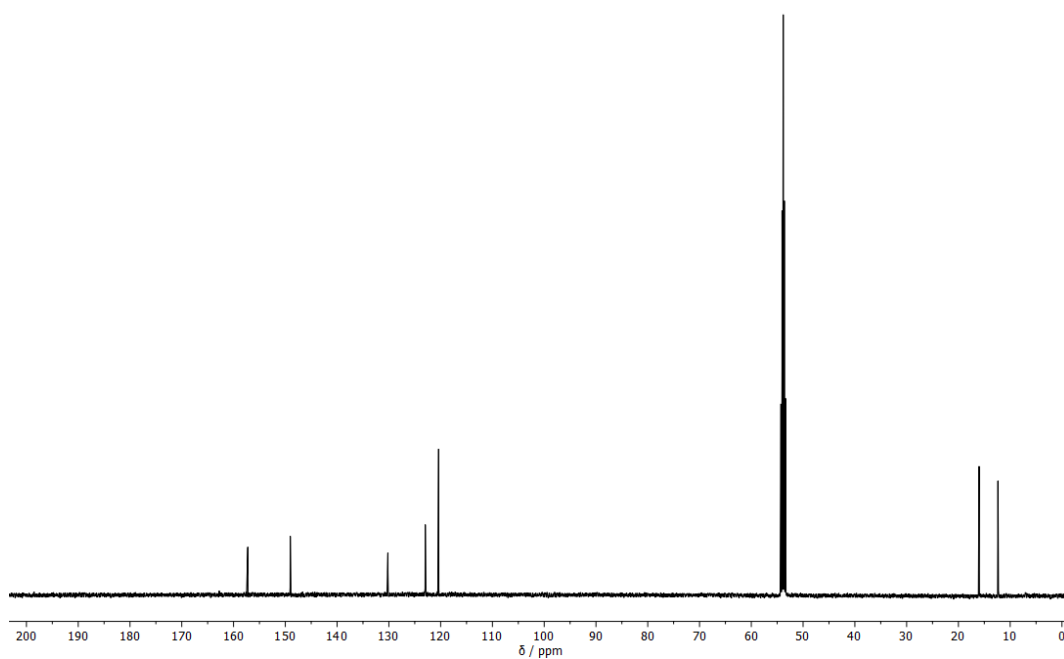
¹H NMR (400 MHz) spectrum of **SBDIPY-1-Cl** in CD₂Cl₂.



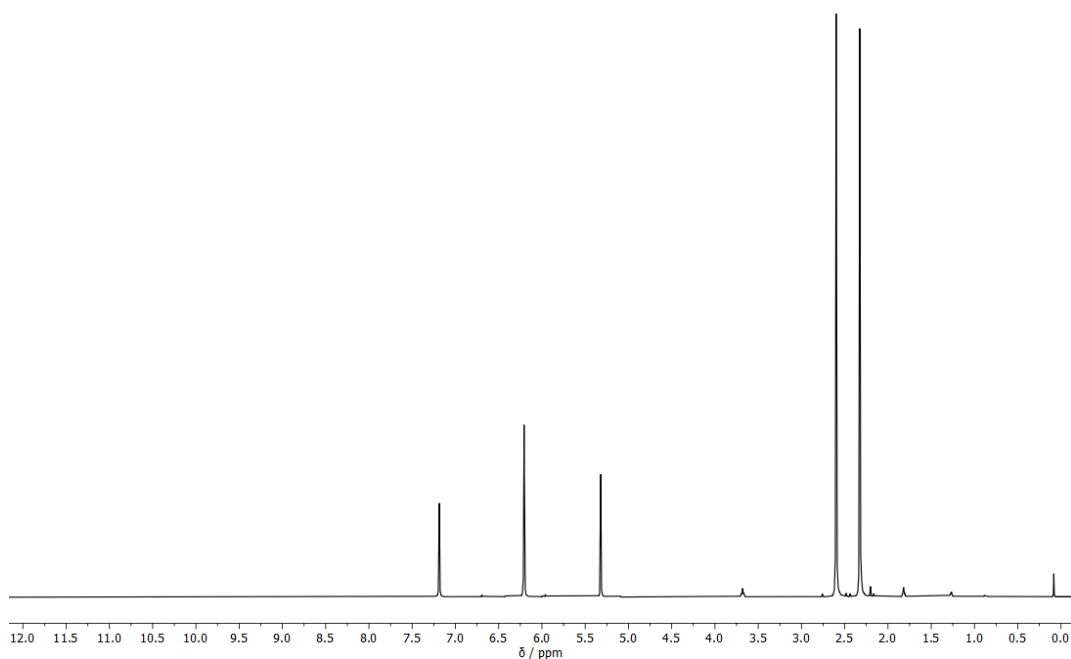
¹³C{¹H} NMR (126 MHz) spectrum of **SBDIPY-1-Cl** in CD₂Cl₂.



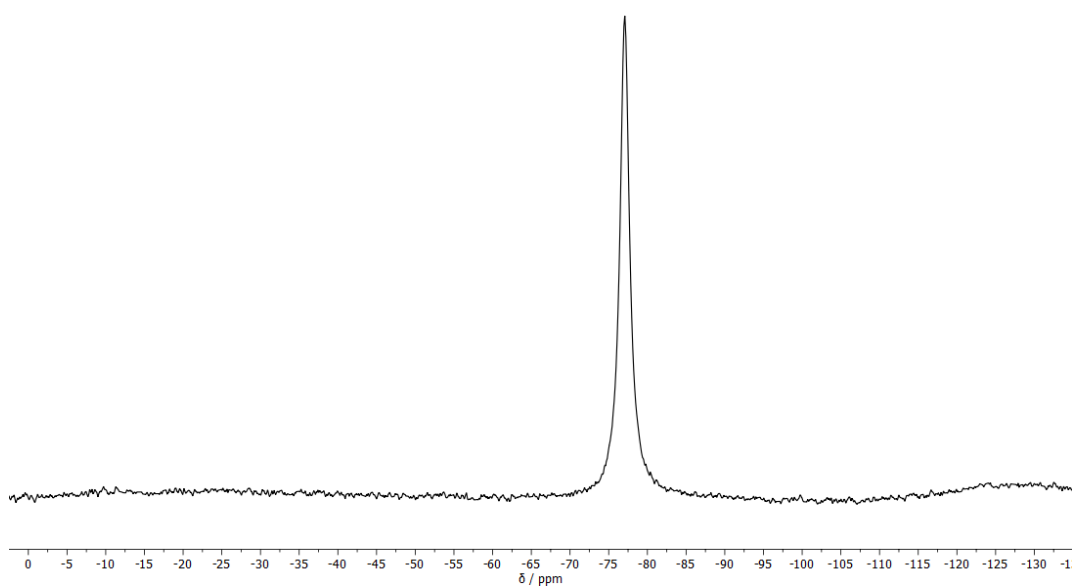
^1H NMR (500 MHz) spectrum of **SBDIPY-1-Br** in CD_2Cl_2 .



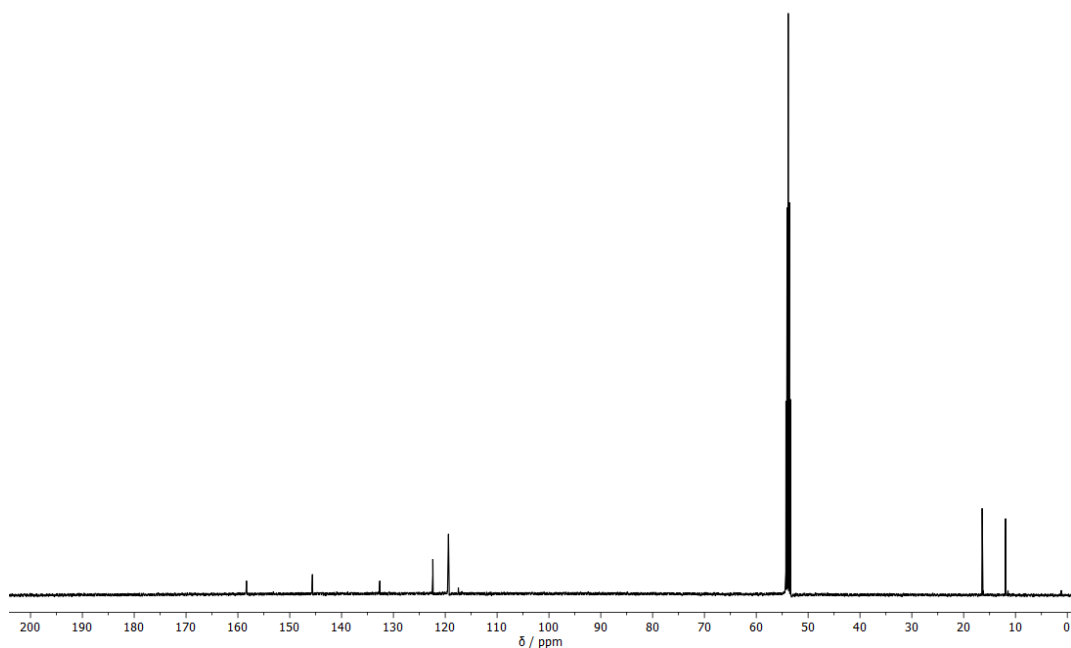
$^{13}\text{C}\{\text{H}\}$ NMR (126 MHz) spectrum of **SBDIPY-1-Br** in CD_2Cl_2 .



^1H NMR (400 MHz) spectrum of **SBDIPY-1-F** in CD_2Cl_2 .



$^{19}\text{F}\{\text{H}\}$ NMR (377 MHz) spectrum of **SBDIPY-1-F** in CD_2Cl_2 .



$^{13}\text{C}\{\text{H}\}$ NMR (126 MHz) spectrum of **SBDIPY-1-F** in CD_2Cl_2 .

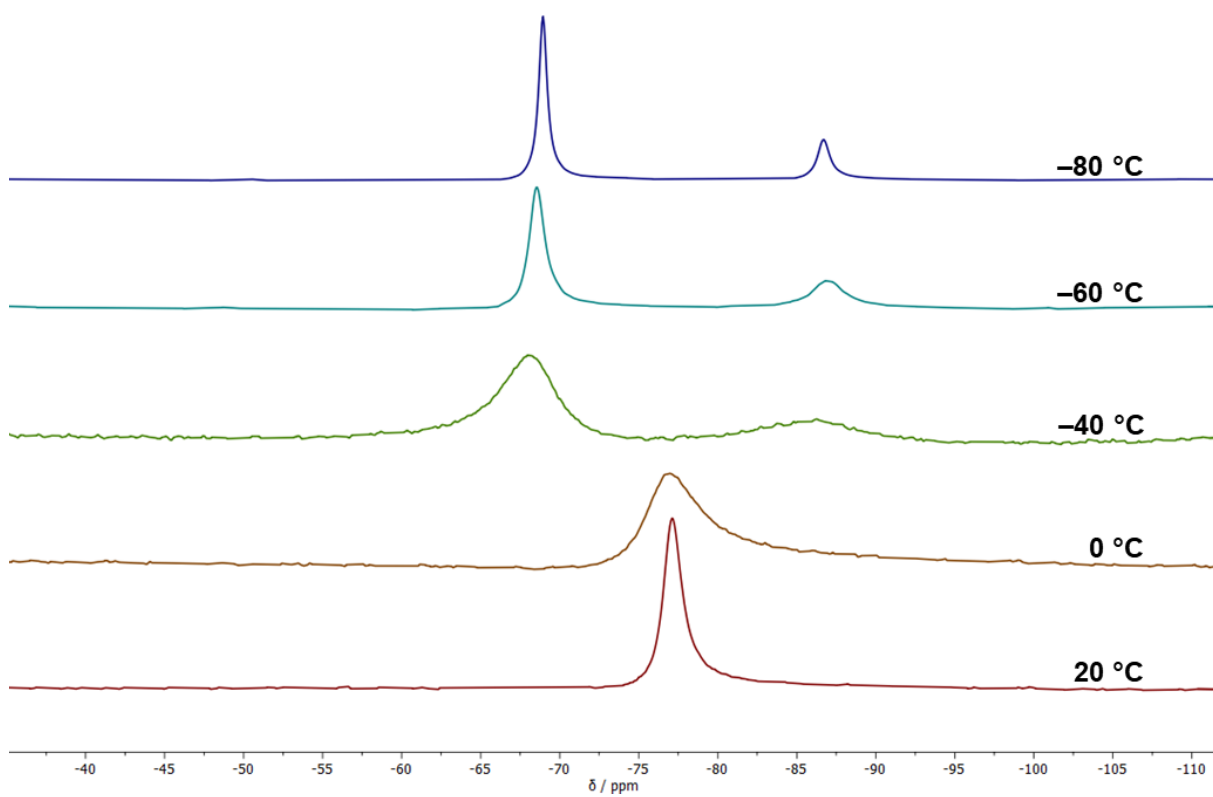
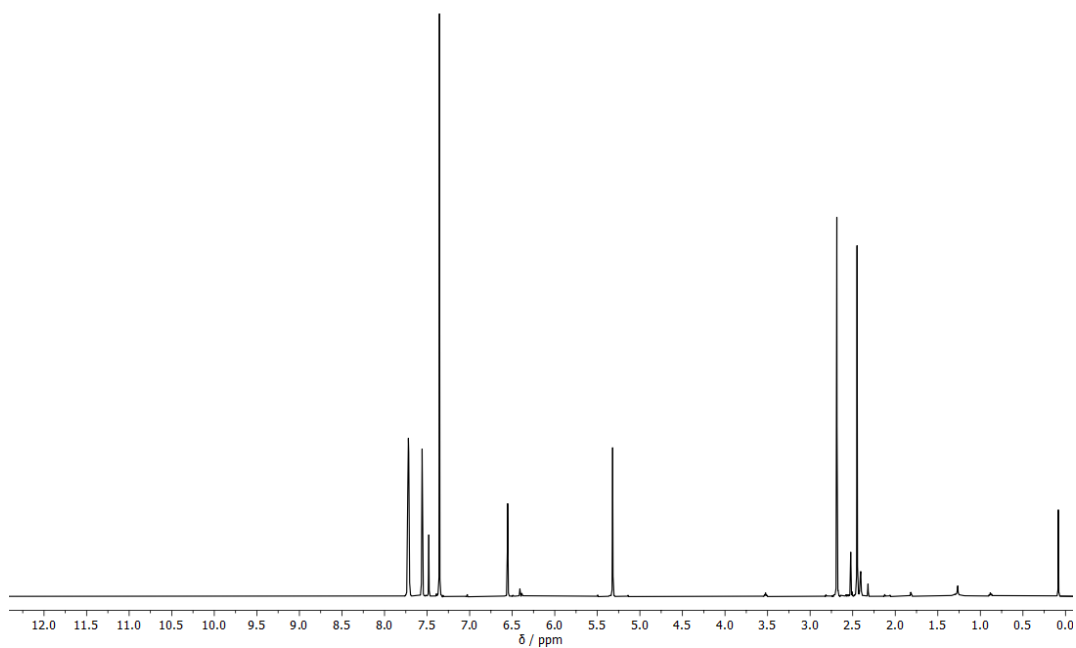
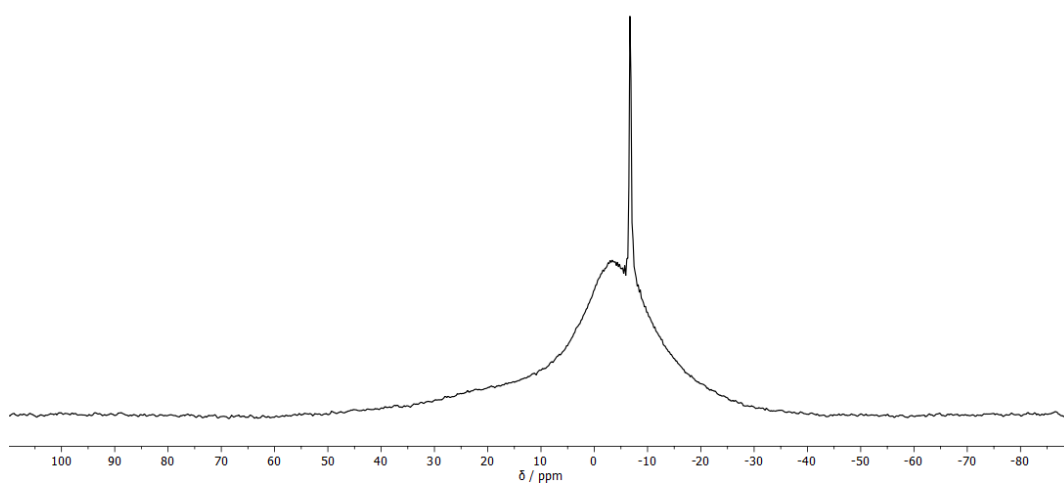


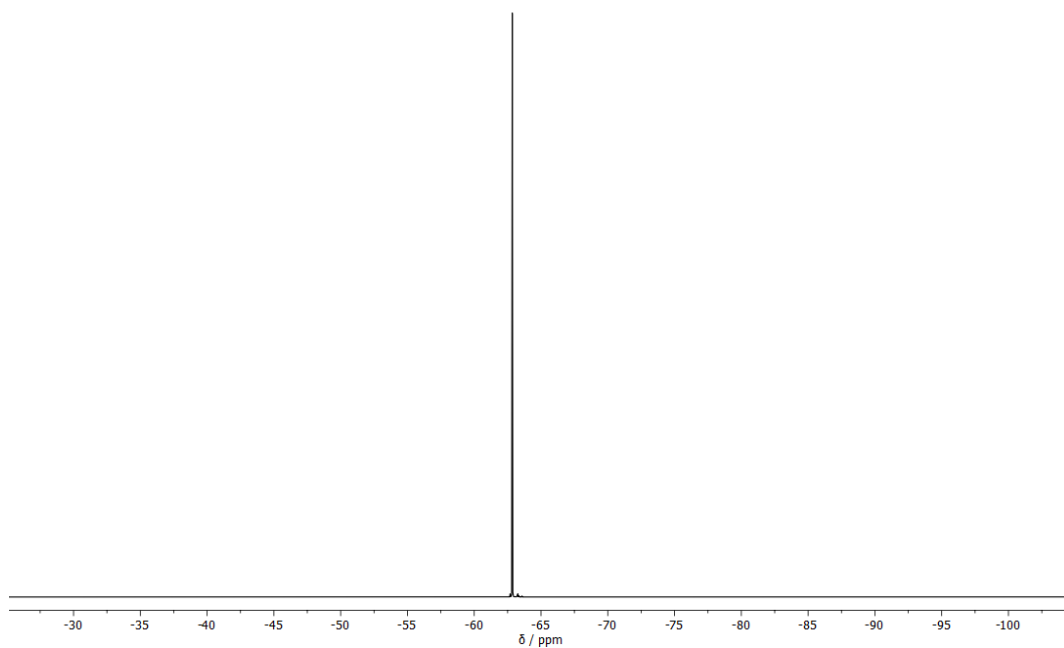
Figure 36: Variable temperature $^{19}\text{F}\{\text{H}\}$ NMR (377 MHz) spectra of **SBDIPY-1-F** in CD_2Cl_2 . Measurement temperatures from top to bottom: $-80\text{ }^\circ\text{C}$, $-60\text{ }^\circ\text{C}$, $-40\text{ }^\circ\text{C}$, $0\text{ }^\circ\text{C}$, $20\text{ }^\circ\text{C}$.



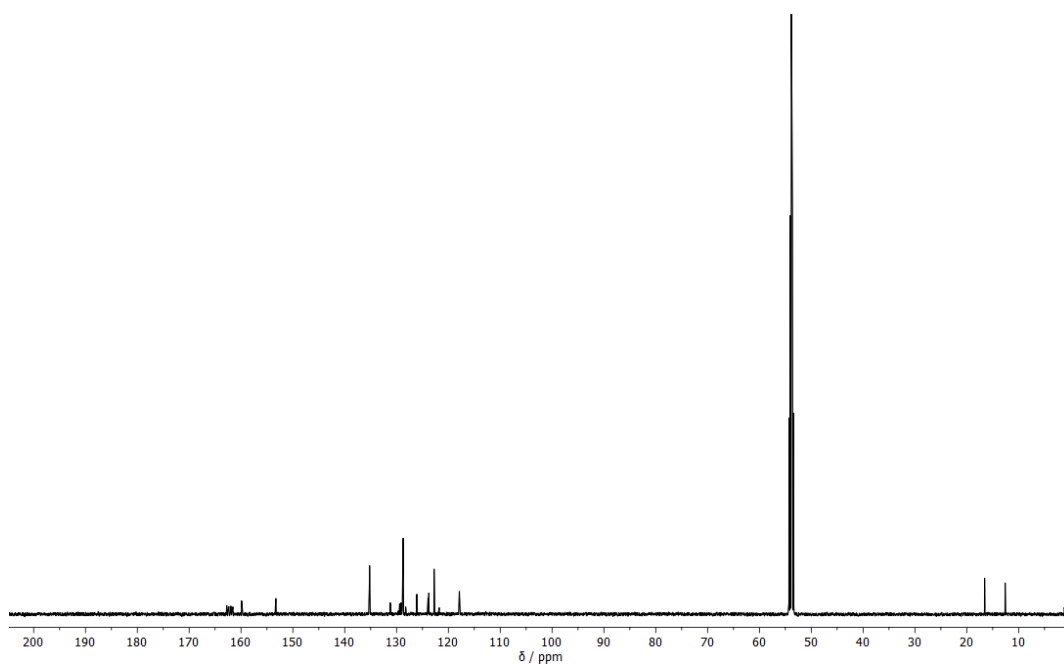
^1H NMR (500 MHz) spectrum of **SBDIPY-1⁺-Cl** in CD_2Cl_2 .



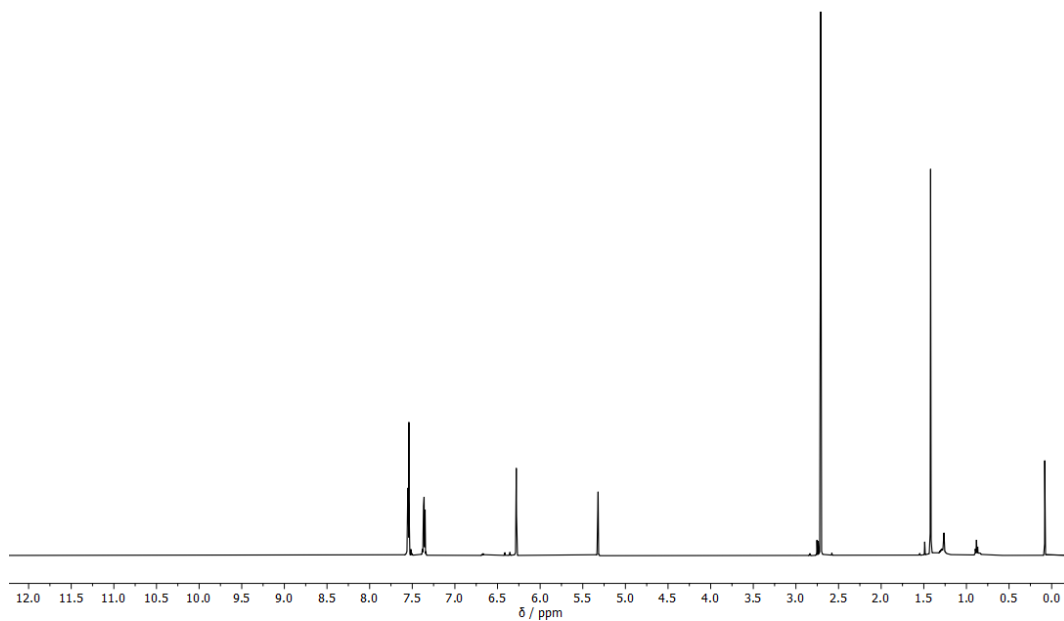
$^{11}\text{B}\{^1\text{H}\}$ NMR (161 MHz) spectrum of **SBDIPY-1⁺-Cl** in CD_2Cl_2 .



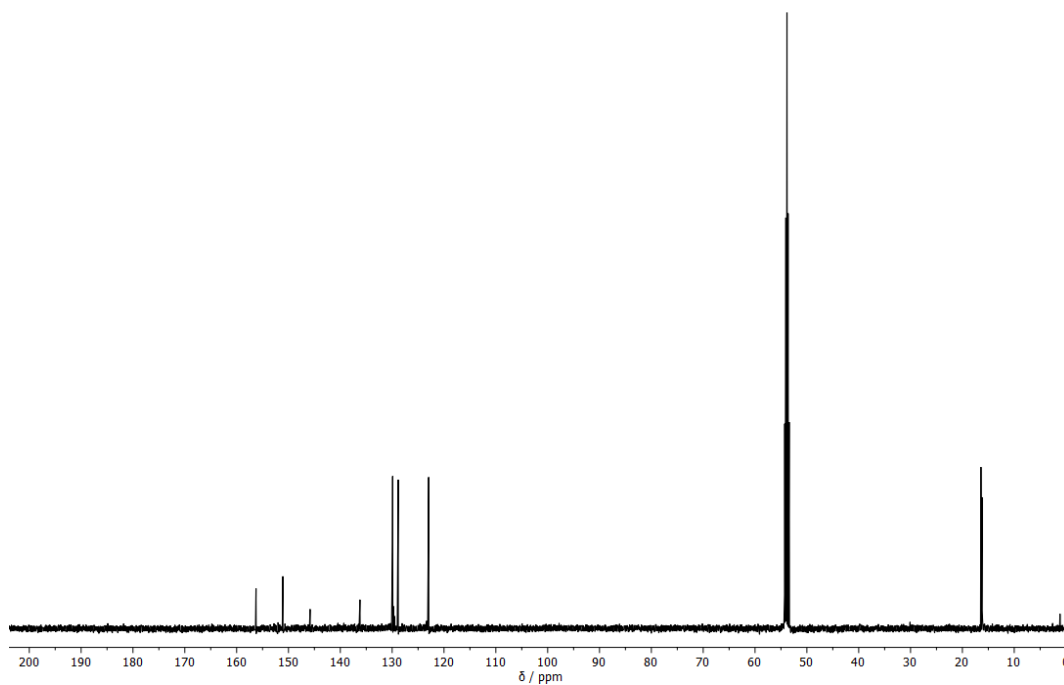
^{19}F NMR (471 MHz) spectrum of **SBDIPY-1⁺-Cl** in CD_2Cl_2 .



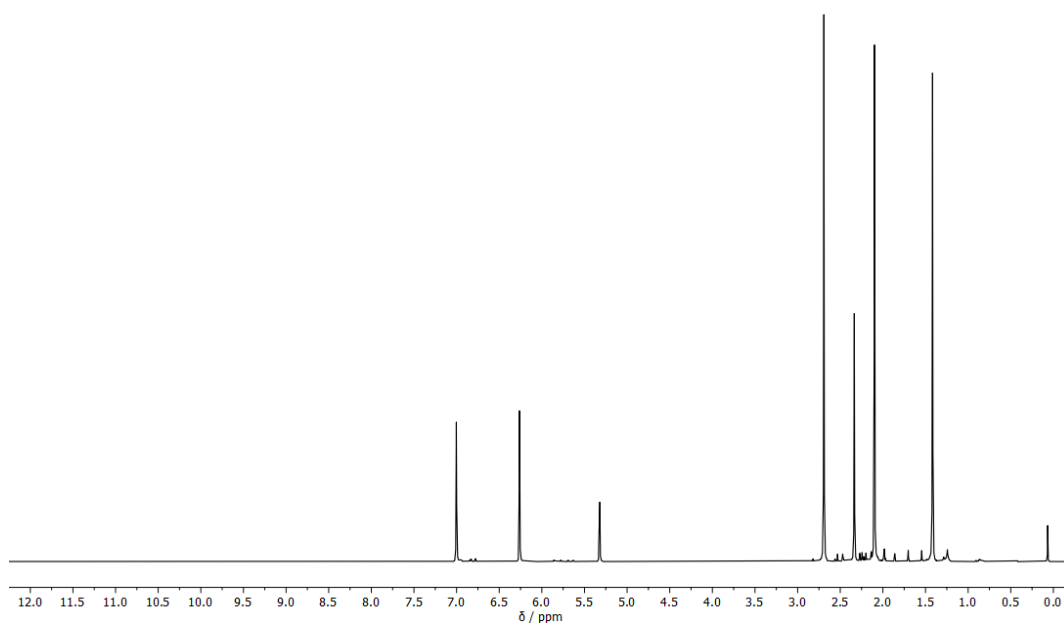
$^{13}\text{C}\{\text{H}\}$ NMR (126 MHz) spectrum of **SBDIPY-1⁺-Cl** in CD_2Cl_2 .



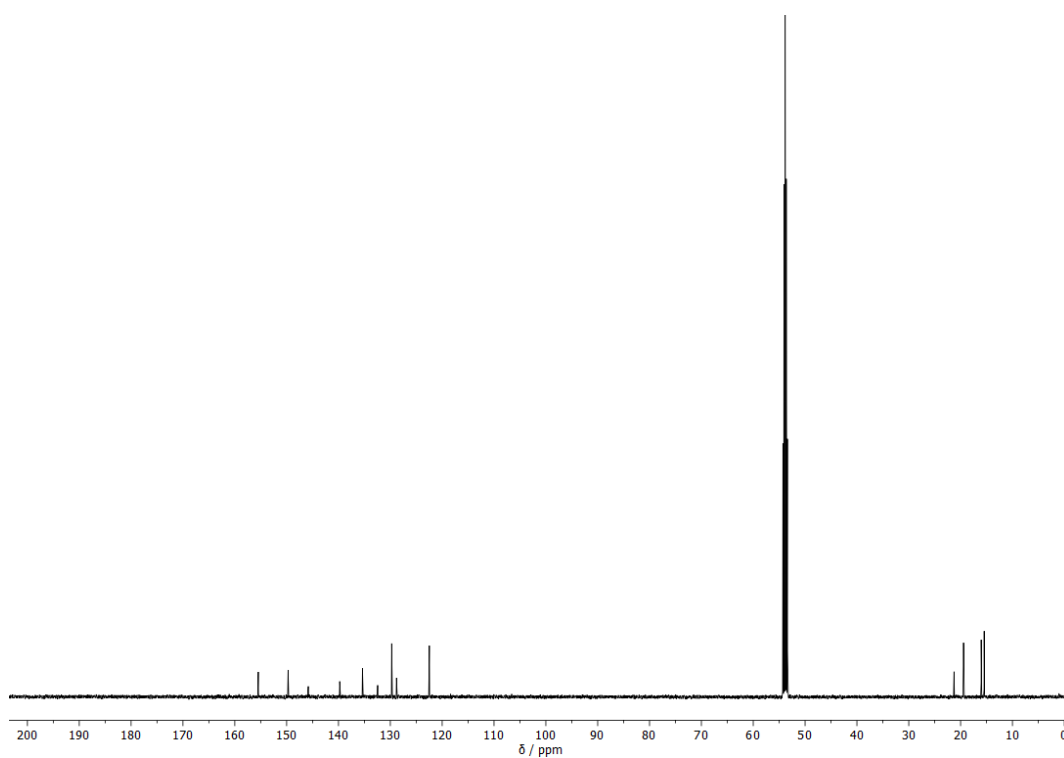
^1H NMR (500 MHz) spectrum of **SBDIPY-2-Cl** in CD_2Cl_2 .



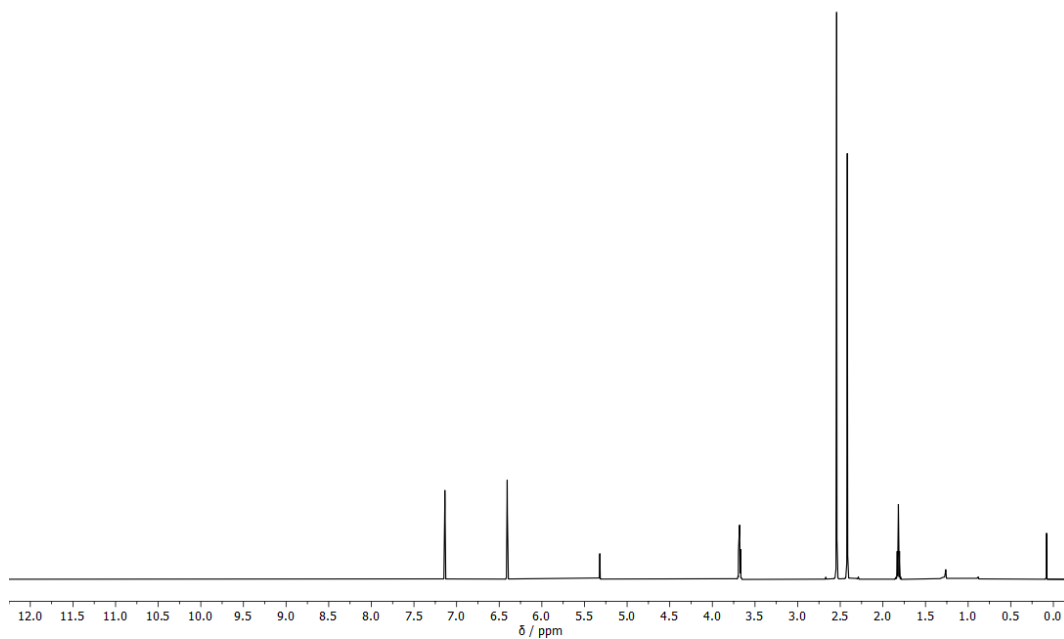
$^{13}\text{C}\{^1\text{H}\}$ NMR (126 MHz) spectrum of **SBDIPY-2-Cl** in CD_2Cl_2 .



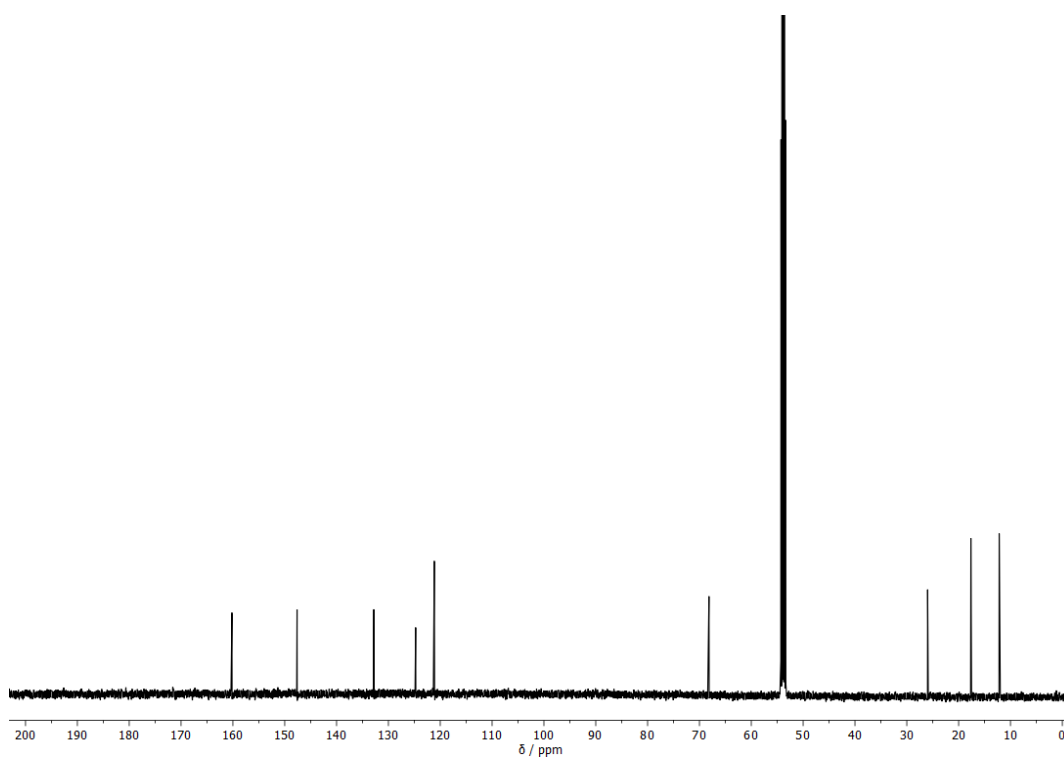
^1H NMR (500 MHz) spectrum of **SBDIPY-3-Cl** in CD_2Cl_2 .



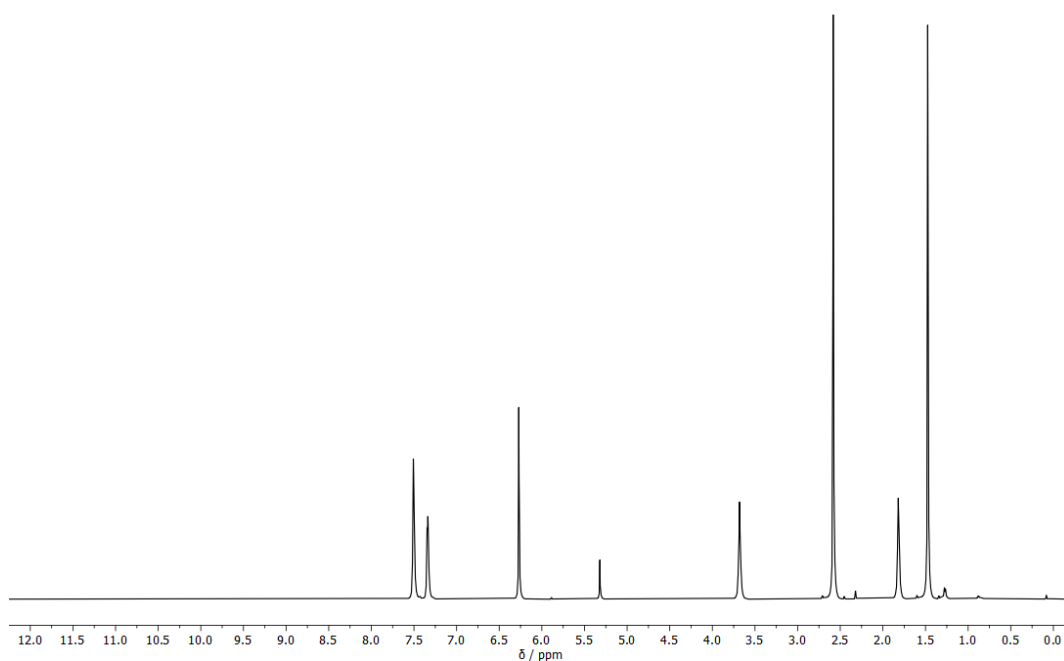
$^{13}\text{C}\{^1\text{H}\}$ NMR (126 MHz) spectrum of **SBDIPY-3-Cl** in CD_2Cl_2 .



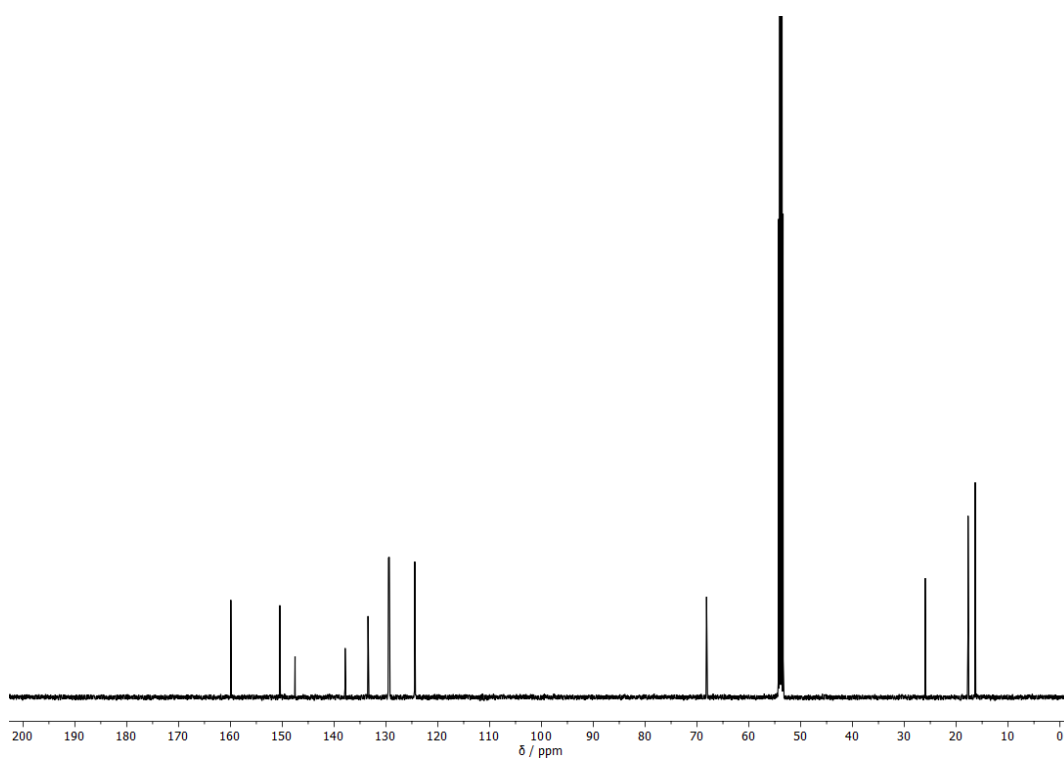
^1H NMR (500 MHz) spectrum of **BIDIPY-1-CI** in CD_2Cl_2 .



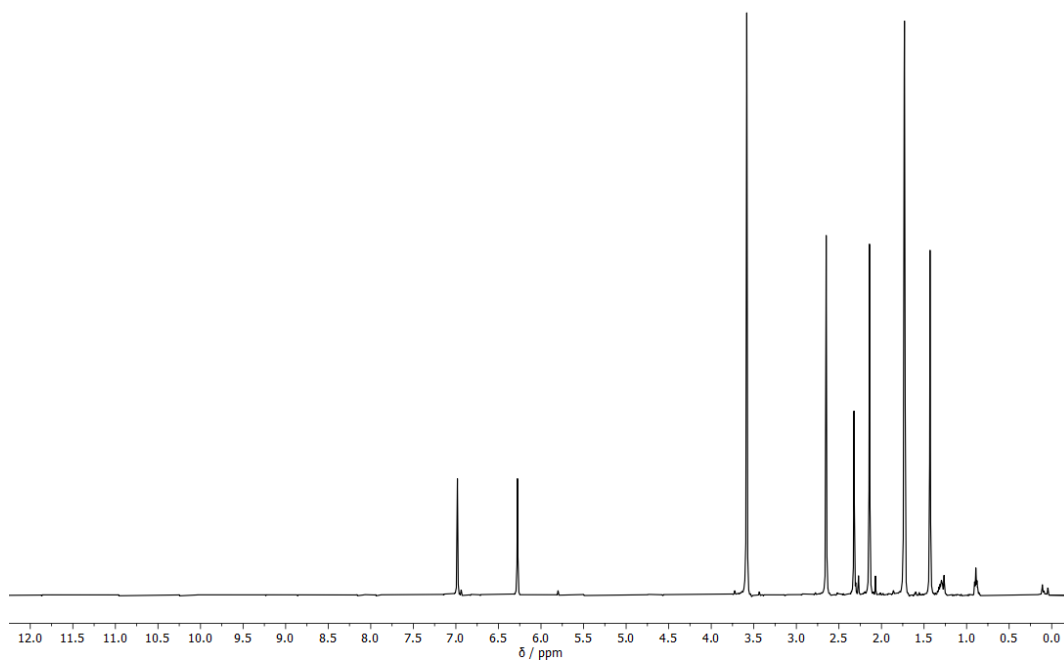
$^{13}\text{C}\{^1\text{H}\}$ NMR (126 MHz) spectrum of **BIDIPY-1-CI** in CD_2Cl_2 .



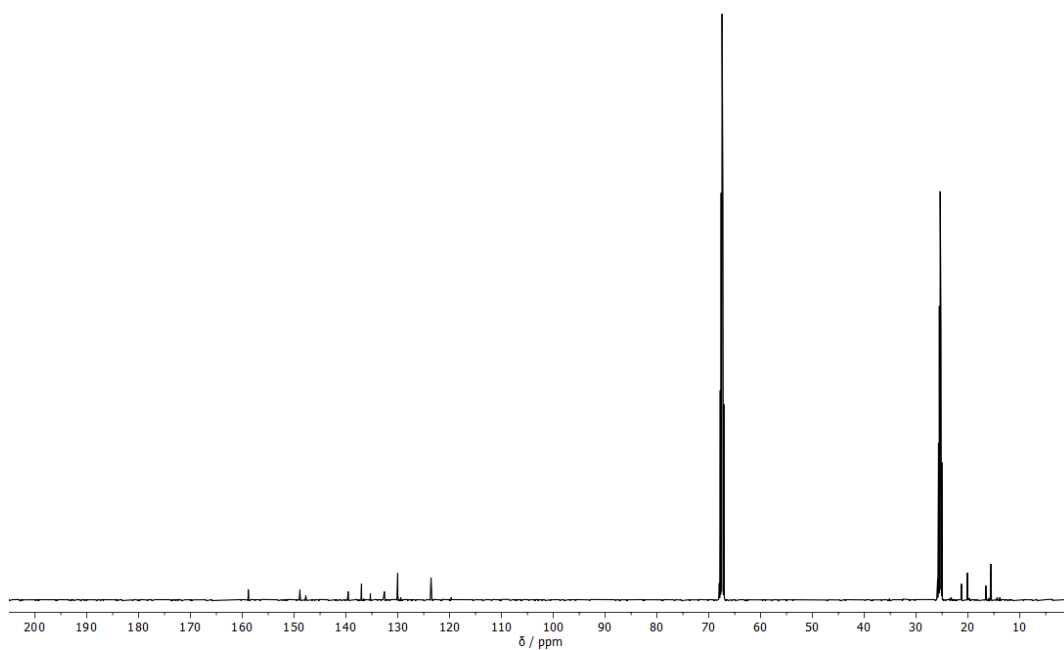
^1H NMR (500 MHz) spectrum of **BIDIPY-2-Cl** in CD_2Cl_2 .



$^{13}\text{C}\{^1\text{H}\}$ NMR (126 MHz) spectrum of **BIDIPY-2-Cl** in CD_2Cl_2 .



¹H NMR (500 MHz) spectrum of **BIDIPY-3-Cl** in THF-*d*₈.



¹³C{¹H} NMR (126 MHz) spectrum of **BIDIPY-3-Cl** in THF-*d*₈.

8. Single crystal X-ray diffraction analysis

8.1. General

Data collection was done on two dual source equipped *Bruker D8 Venture* four-circle-diffractometer from *Bruker AXS GmbH*; used X-ray sources: microfocus $\mu\text{S } 2.0$ Cu/Mo and microfocus $\mu\text{S } 3.0$ Ag/Mo from *Incoatec GmbH* with mirror optics *HELIOS* and single-hole collimator from *Bruker AXS GmbH*; used detector: *Photon III CE14* (Cu/Mo) and *Photon III HE* (Ag/Mo) from *Bruker AXS GmbH*.

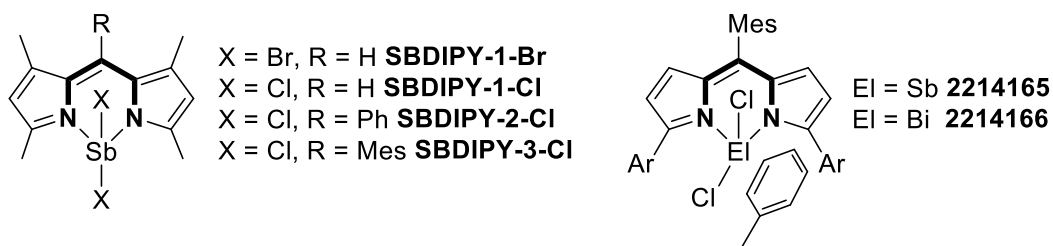
Used programs: *APEX4 Suite* (v2022.1-1) for data collection and therein integrated programs *SAINT V8.40A* (Integration) und *SADABS 2016/2* (Absorption correction) from *Bruker AXS GmbH*; structure solution was done with *SHELXT*^[13], refinement with *SHELXL-2018/3*^[13] *OLEX*² and *FinalCif* were used for data finalization.^[14,15]

Special Utilities: *SMZ1270* stereomicroscope from *Nikon Metrology GmbH* was used for sample preparation; crystals were mounted on *MicroMounts* or *MicroLoops* from *MiTeGen* in NVH oil; for sensitive samples the *X-TEMP 2 System* was used for picking of crystals^[16]; crystals were cooled to given temperature with *Cryostream 800* from *Oxford Cryosystems*.

8.2. Comparison of geometric features in solid-state

The structurally related solid-state structures of **SBDIPY-1-Cl**, **SBDIPY-2-Cl**, **SBDIPY-3-Cl** and **SBDIPY-1-Br** were analysed and compared to the structures reported by Liu *et al.*^[17], revealing notable geometric features. The X1–E1–X2 angle in all the **SBDIPY** compounds are close to 170°, while the coordination of toluene causes a distortion to smaller angles. Exchange of the chlorides with bromides causes a minor increase in X1–E1–X2 angle. The herein reported structures, all feature two different Sb–Cl bonds while the E1–X distances of the structures reported by Liu and co-workers are the same.^[17] Another noticeable difference is in the E1–N lengths as well as the N···N distances, most likely due to the lack of coordinating toluene molecule. Finally, the distortion of the central heterocycle in terms of bending at the heavier pnictogen corner is compared by distance to the heterocyclic mean plane. The observed differences are striking, especially between **SBDIPY-1-Cl**, that is mostly flat, and **SBDIPY-1-Br**, that features the most distortion of all structures. An explanation for this geometric differences is only found when scrutinizing the intermolecular interactions, in the case of **SBDIPY-1-Cl** Sb···Cl distances of 3.714 Å, and for the corresponding bromo 3.781 Å are found, which are both considerably shorter than the sum of Van der Waals radii (4.29 and 4.33 Å, respectively).^[18]

Table 5: Selected bond lengths and angles for heavier analogues of BODIPY reported in this study and literature.^[17] Mean plane (MPLN) defined by the atoms drawn bold.



	X1–El–X2 [°]	N1–El–N2 [°]	El–X1 [Å]	El–X2 [Å]	El–N1 [Å]	El–N2 [Å]	MPLN···El [Å]	N···N [Å]
SBDIPY-1-Br	175.2(1)	86.4(1)	2.746(1)	2.719(1)	2.085(2)	2.082(2)	0.410	2.852
SBDIPY-1-Cl	170.7(1)	88.2(1)	2.589(1)	2.530(1)	2.086(1)	2.079(1)	0.053	2.898
SBDIPY-2-Cl	170.1(1)	88.0(1)	2.583(1)	2.520(1)	2.059(1)	2.063(1)	0.102	2.864
SBDIPY-3-Cl	171.1(1)	87.4(1)	2.574(1)	2.537(1)	2.063(1)	2.055(1)	0.261	2.844
2214165	161.0(1)	89.0(1)	2.538(2)	2.534(2)	2.120(5)	2.102(5)	0.059	2.955
2214166	163.0(1)	85.7(1)	2.633(1)	2.620(1)	2.220(2)	2.224(2)	0.062	3.021

8.3. Refinement details

SBDIPY-1-F

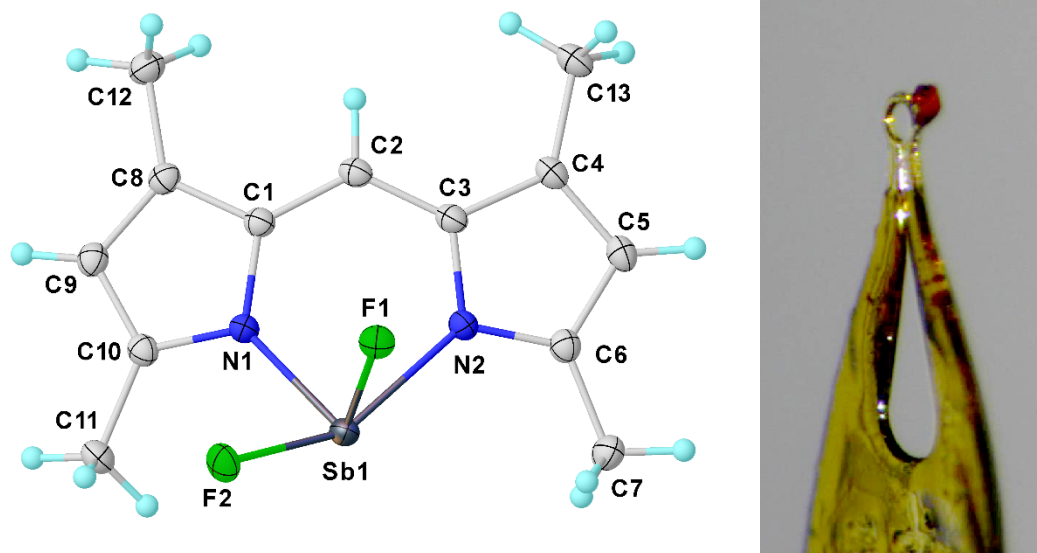


Figure 37: Full asymmetric unit and labeling scheme for **SBDIPY-1-F**. Displacement ellipsoids are drawn at 50% probability level. The crystals were obtained from a mixture of THF and hexane.

CCDC number	2241582
Empirical formula	C ₁₃ H ₁₅ F ₂ N ₂ Sb
Formula weight	359.02
Temperature [K]	100.00
Crystal system	triclinic
Space group (number)	$P\bar{1}$ (2)
<i>a</i> [Å]	8.0025(9)
<i>b</i> [Å]	8.9517(8)
<i>c</i> [Å]	9.5870(10)
α [°]	68.099(4)

β [°]	79.046(4)
γ [°]	82.806(3)
Volume [Å ³]	624.49(11)
<i>Z</i>	2
ρ_{calc} [gcm ⁻³]	1.909
μ [mm ⁻¹]	2.217
<i>F</i> (000)	352
Crystal size [mm ³]	0.096×0.079×0.028
Crystal colour	red
Crystal shape	block
Radiation	MoK α (λ =0.71073 Å)

2 θ range [°]	4.64 to 61.05 (0.70 Å)
Index ranges	-11 ≤ h ≤ 11 -12 ≤ k ≤ 12 -13 ≤ l ≤ 13
Reflections collected	18096
Independent reflections	3824 $R_{\text{int}} = 0.0297$ $R_{\text{sigma}} = 0.0235$
Completeness to $\theta = 25.242^\circ$	100.0%

Data / Restraints / Parameters	3824/0/167
Goodness-of-fit on F^2	1.081
Final R indexes [$\geq 2\sigma(I)$]	$R_1 = 0.0194$ $wR_2 = 0.0446$
Final R indexes [all data]	$R_1 = 0.0225$ $wR_2 = 0.0460$
Largest peak/hole [$\text{e}\text{\AA}^{-3}$]	0.63/-0.37

SBDIPY-1-Cl

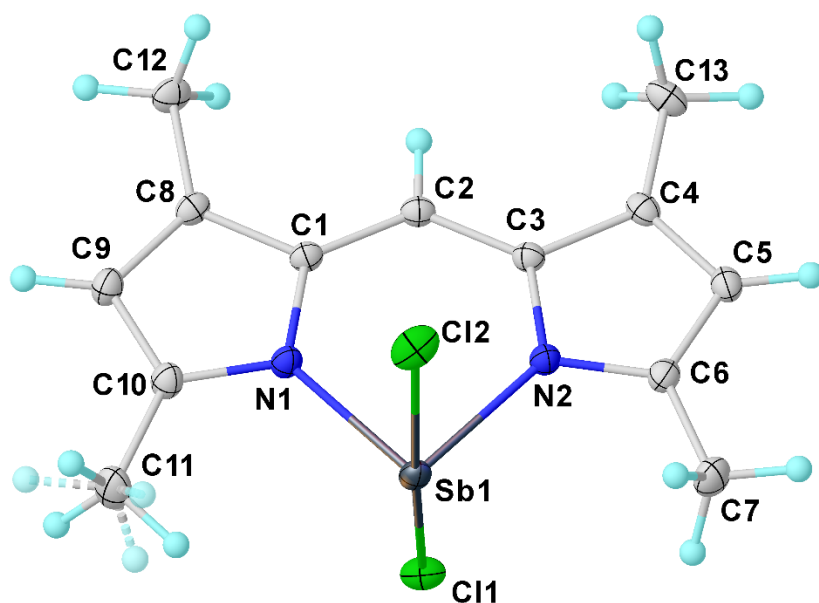


Figure 38: Full asymmetric unit and labeling scheme for **SBDIPY-1-Cl**. Displacement ellipsoids are drawn at 50% probability level. Disordered molecule part minors drawn translucent with stippled bonds. The crystals were obtained from a mixture of THF and hexane.

CCDC number	2241590
Empirical formula	C ₁₃ H ₁₅ Cl ₂ N ₂ Sb
Formula weight	391.92
Temperature [K]	100.00
Crystal system	monoclinic
Space group (number)	<i>P</i> 2 ₁ / <i>c</i> (14)
<i>a</i> [Å]	10.7292(5)
<i>b</i> [Å]	9.9358(6)
<i>c</i> [Å]	13.9550(7)
α [°]	90

β [°]	91.646(2)
γ [°]	90
Volume [Å ³]	1487.03(14)
<i>Z</i>	4
ρ_{calc} [gcm ⁻³]	1.751
μ [mm ⁻¹]	2.199
<i>F</i> (000)	768
Crystal size [mm ³]	0.149×0.119×0.111
Crystal colour	red
Crystal shape	block
Radiation	MoK α (λ =0.71073 Å)

2 Θ range [°]	3.80 to 71.19 (0.61 Å)
Index ranges	-17 ≤ h ≤ 17 -16 ≤ k ≤ 16 -22 ≤ l ≤ 22
Reflections collected	67080
Independent reflections	6547 $R_{\text{int}} = 0.0193$ $R_{\text{sigma}} = 0.0101$
Completeness to $\Theta = 25.242^\circ$	99.9%

Data / Restraints / Parameters	6547/4/168
Goodness-of-fit on F^2	1.094
Final R indexes [$\geq 2\sigma(I)$]	$R_1 = 0.0151$ $wR_2 = 0.0368$
Final R indexes [all data]	$R_1 = 0.0176$ $wR_2 = 0.0379$
Largest peak/hole [$\text{e}\text{\AA}^{-3}$]	0.54/-0.40

SBDIPY-1-Br

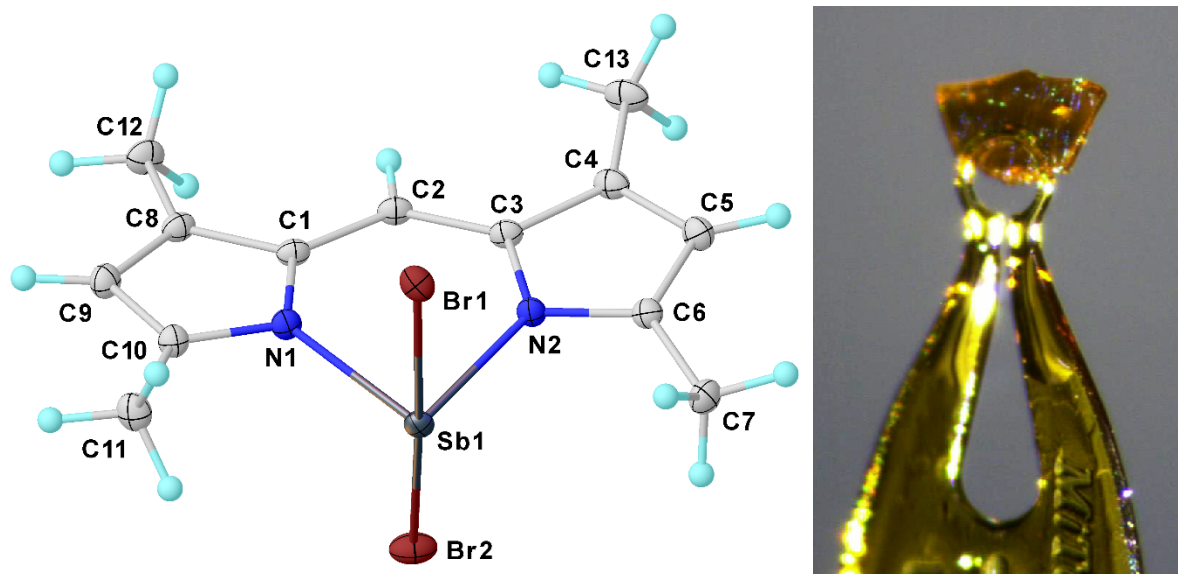


Figure 39: Full asymmetric unit and labeling scheme for **SBDIPY-1-Br**. Displacement ellipsoids are drawn at 50% probability level. The structure was refined as an ideal inversion twin, with a final batch scale factor of 0.164(4). The crystals were obtained from a mixture of THF and hexane.

CCDC number	2241583
Empirical formula	C ₁₃ H ₁₅ Br ₂ N ₂ Sb
Formula weight	480.84
Temperature [K]	100.00
Crystal system	monoclinic
Space group (number)	<i>Cc</i> (9)
<i>a</i> [Å]	17.2704(8)
<i>b</i> [Å]	12.0396(6)
<i>c</i> [Å]	7.6022(3)
α [°]	90
β [°]	108.934(2)

γ [°]	90
Volume [Å ³]	1495.19(12)
<i>Z</i>	4
ρ_{calc} [gcm ⁻³]	2.136
μ [mm ⁻¹]	7.175
<i>F</i> (000)	912
Crystal size [mm ³]	0.394×0.209×0.02
Crystal colour	yellow
Crystal shape	plate
Radiation	MoK α (λ =0.71073 Å)
2 θ range [°]	4.20 to 68.17 (0.63 Å)

Index ranges	-27 ≤ h ≤ 27 -18 ≤ k ≤ 17 -11 ≤ l ≤ 11
Reflections collected	49573
Independent reflections	5708 $R_{\text{int}} = 0.0238$ $R_{\text{sigma}} = 0.0131$
Completeness to $\theta = 25.242^\circ$	100.0%
Data / Restraints / Parameters	5708/2/168

Goodness-of-fit on F^2	1.033
Final R indexes [$\geq 2\sigma(I)$]	$R_1 = 0.0137$ $wR_2 = 0.0330$
Final R indexes [all data]	$R_1 = 0.0141$ $wR_2 = 0.0332$
Largest peak/hole [$\text{e}\text{\AA}^{-3}$]	0.31/-0.45
Flack X parameter	0.164(4)

SBDIPY-1⁺-Cl

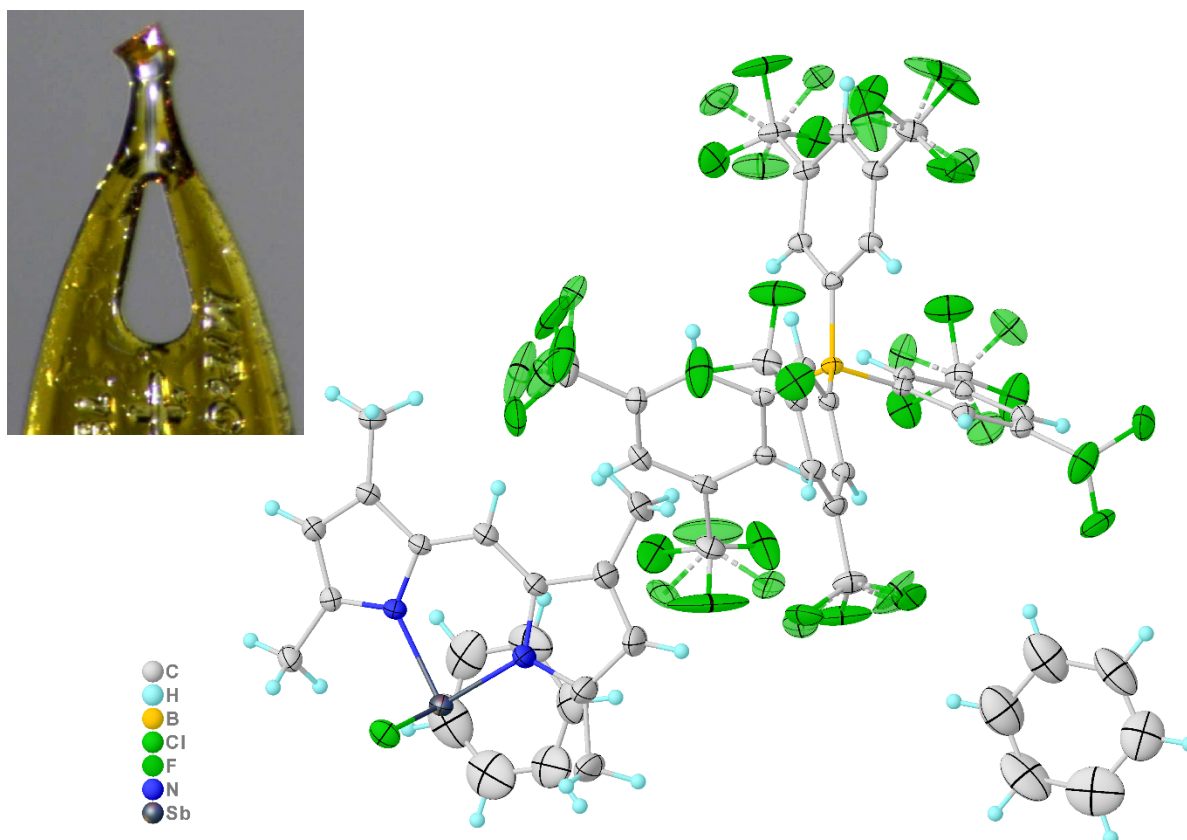


Figure 40: Full asymmetric unit for **SBDIPY-1⁺-Cl**. Displacement ellipsoids are drawn at 50% probability level. Disordered molecule part minors drawn translucent with stippled bonds. The crystals were obtained from a mixture of benzene and CH₂Cl₂.

CCDC number	2241589
Empirical formula	C ₅₄ H ₃₆ BClF ₂₄ N ₂ Sb
Formula weight	1336.86
Temperature [K]	100.00
Crystal system	triclinic
Space group (number)	$P\bar{1}$ (2)
<i>a</i> [Å]	12.379(4)

<i>b</i> [Å]	12.587(4)
<i>c</i> [Å]	18.983(6)
α [°]	79.607(7)
β [°]	75.288(7)
γ [°]	80.032(7)
Volume [Å ³]	2788.7(14)
<i>Z</i>	2
ρ_{calc} [gcm ⁻³]	1.592

μ [mm ⁻¹]	0.661
$F(000)$	1326
Crystal size [mm ³]	0.135×0.114×0.043
Crystal colour	orange
Crystal shape	plate
Radiation	MoK α ($\lambda=0.71073$ Å)
2 θ range [°]	4.26 to 55.92 (0.76 Å)
Index ranges	-15 ≤ h ≤ 16 -16 ≤ k ≤ 16 -24 ≤ l ≤ 24
Reflections collected	84600

Independent reflections	13335 $R_{\text{int}} = 0.0577$ $R_{\text{sigma}} = 0.0402$
Completeness to $\theta = 25.242^\circ$	99.9%
Data / Restraints / Parameters	13335/161/947
Goodness-of-fit on F^2	1.068
Final R indexes [$I \geq 2\sigma(I)$]	$R_1 = 0.0445$ $wR_2 = 0.1123$
Final R indexes [all data]	$R_1 = 0.0569$ $wR_2 = 0.1195$
Largest peak/hole [eÅ ⁻³]	0.96/-0.98

SBDIPY-2-Cl

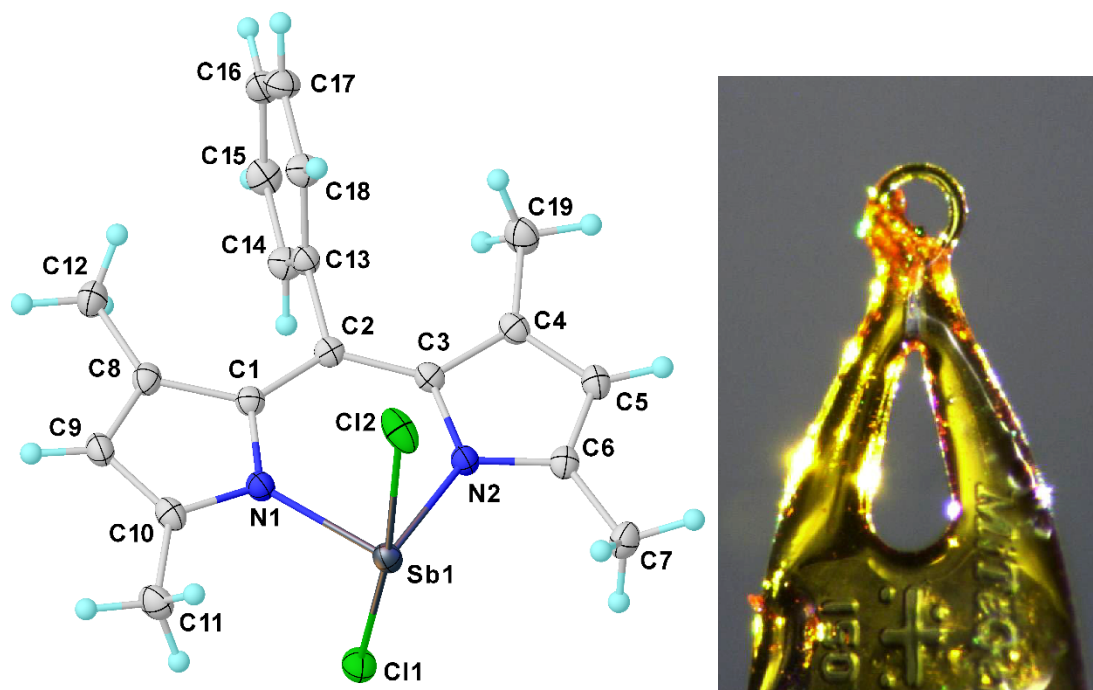


Figure 41: Full asymmetric unit and labeling scheme for **SBDIPY-2-Cl**. Displacement ellipsoids are drawn at 50% probability level. The crystals were obtained from a mixture of THF and hexane.

CCDC number	2241588
Empirical formula	C ₁₉ H ₁₉ Cl ₂ N ₂ Sb
Formula weight	468.01
Temperature [K]	100.00
Crystal system	monoclinic
Space group (number)	<i>P</i> 2 ₁ / <i>n</i> (14)
<i>a</i> [Å]	12.4279(6)
<i>b</i> [Å]	7.8441(4)
<i>c</i> [Å]	19.0889(10)
α [°]	90

β [°]	96.771(2)
γ [°]	90
Volume [Å ³]	1847.92(16)
<i>Z</i>	4
ρ_{calc} [gcm ⁻³]	1.682
μ [mm ⁻¹]	1.785
<i>F</i> (000)	928
Crystal size [mm ³]	0.183×0.09×0.034
Crystal colour	orange
Crystal shape	plate

Radiation	MoK α ($\lambda=0.71073$ Å)
2 Θ range [°]	4.15 to 61.12 (0.70 Å)
Index ranges	-17 \leq h \leq 17 -11 \leq k \leq 9 -27 \leq l \leq 27
Reflections collected	45683
Independent reflections	5660 $R_{\text{int}} = 0.0310$ $R_{\text{sigma}} = 0.0188$

Completeness to $\Theta = 25.242^\circ$	100.0%
Data / Restraints / Parameters	5660/0/221
Goodness-of-fit on F^2	1.063
Final R indexes [$I \geq 2\sigma(I)$]	$R_1 = 0.0224$ $wR_2 = 0.0461$
Final R indexes [all data]	$R_1 = 0.0288$ $wR_2 = 0.0487$
Largest peak/hole [eÅ $^{-3}$]	0.49/-0.53

SBDIPY-3-Cl

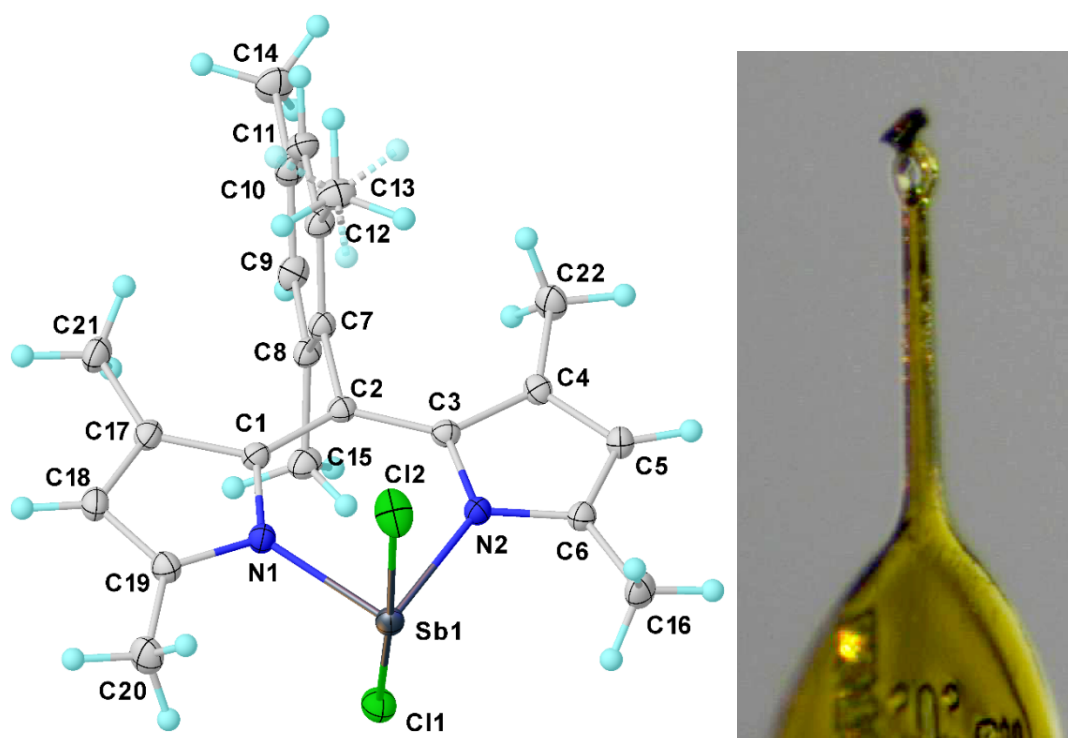


Figure 42: Full asymmetric unit and labeling scheme for **SBDIPY-3-Cl**. Displacement ellipsoids are drawn at 50% probability level. Disordered molecule part minors drawn translucent with stippled bonds. The crystals were obtained from a mixture of THF and hexane.

CCDC number	2241584
Empirical formula	C ₂₂ H ₂₅ Cl ₂ N ₂ Sb
Formula weight	510.09
Temperature [K]	100.00
Crystal system	triclinic
Space group (number)	$P\bar{1}$ (2)
<i>a</i> [Å]	7.7567(9)
<i>b</i> [Å]	11.3335(15)
<i>c</i> [Å]	13.6924(17)

α [°]	65.998(3)
β [°]	80.920(3)
γ [°]	76.814(3)
Volume [Å ³]	1067.8(2)
<i>Z</i>	2
ρ_{calc} [gcm ⁻³]	1.587
μ [mm ⁻¹]	1.552
<i>F</i> (000)	512
Crystal size [mm ³]	0.078×0.077×0.048
Crystal colour	orange

Crystal shape	block
Radiation	MoK α ($\lambda=0.71073$ Å)
2 Θ range [°]	4.07 to 59.31 (0.72 Å)
Index ranges	-10 \leq h \leq 10 -15 \leq k \leq 15 -19 \leq l \leq 19
Reflections collected	65221
Independent reflections	6011 $R_{\text{int}} = 0.0322$ $R_{\text{sigma}} = 0.0144$

Completeness to $\Theta = 25.242^\circ$	99.9%
Data / Restraints / Parameters	6011/0/252
Goodness-of-fit on F^2	1.078
Final R indexes [$I \geq 2\sigma(I)$]	$R_1 = 0.0178$ $wR_2 = 0.0446$
Final R indexes [all data]	$R_1 = 0.0196$ $wR_2 = 0.0455$
Largest peak/hole [$e\text{\AA}^{-3}$]	0.68/-0.42

BIDIPY-1-Cl

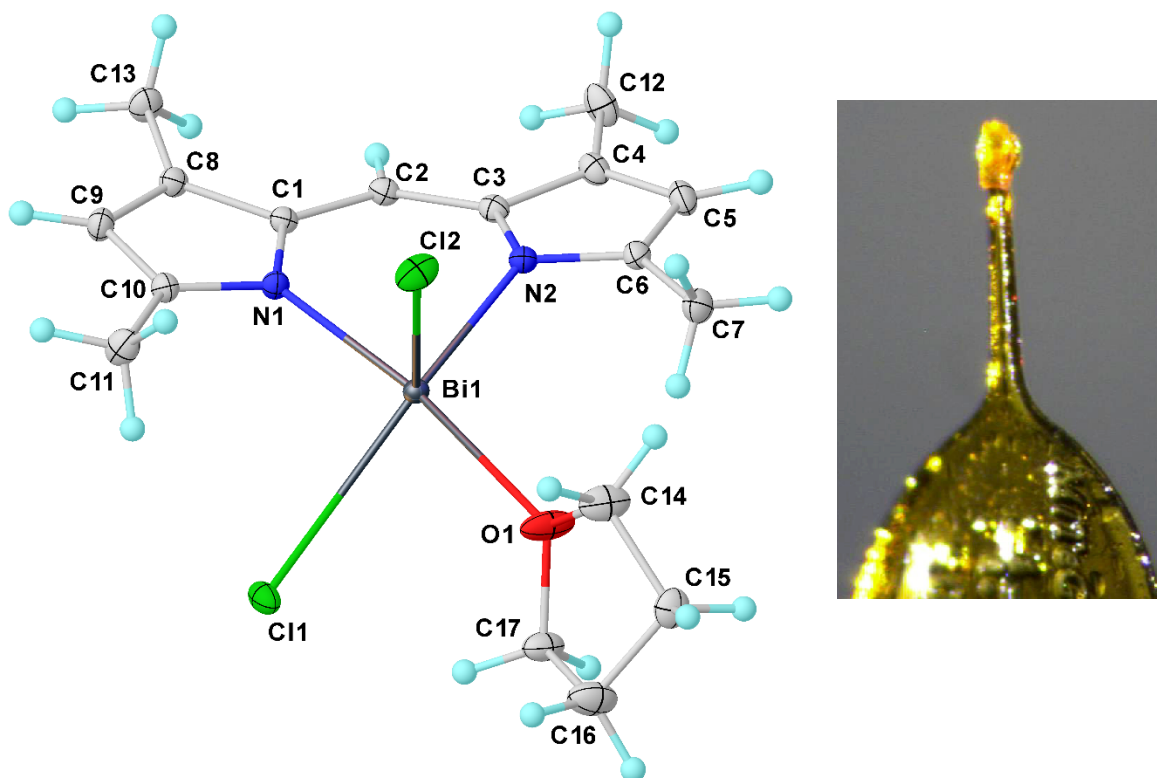


Figure 43: Full asymmetric unit and labeling scheme for **BIDIPY-1-Cl**. Displacement ellipsoids are drawn at 50% probability level. The crystals were obtained from a mixture of THF and hexane.

CCDC number	2241585
Empirical formula	$C_{34}H_{46}Bi_2Cl_4N_4O_2$
Formula weight	1102.51
Temperature [K]	100.00
Crystal system	monoclinic
Space group (number)	$P2_1/c$ (14)
a [Å]	8.7403(9)
b [Å]	9.2435(6)

c [Å]	22.984(3)
α [°]	90
β [°]	95.441(4)
γ [°]	90
Volume [Å ³]	1848.5(3)
Z	2
ρ_{calc} [gcm ⁻³]	1.981
μ [mm ⁻¹]	9.832
$F(000)$	1056

Crystal size [mm ³]	0.156×0.074×0.034
Crystal colour	orange
Crystal shape	block
Radiation	MoK α ($\lambda=0.71073$ Å)
2 θ range [°]	4.68 to 67.51 (0.64 Å)
Index ranges	-13 ≤ h ≤ 13 -14 ≤ k ≤ 14 -35 ≤ l ≤ 35
Reflections collected	46052
Independent reflections	6909 $R_{\text{int}} = 0.0337$ $R_{\text{sigma}} = 0.0241$

Completeness to $\theta = 25.242^\circ$	100.0%
Data / Restraints / Parameters	6909/0/212
Goodness-of-fit on F^2	1.044
Final R indexes [$I \geq 2\sigma(I)$]	$R_1 = 0.0187$ $wR_2 = 0.0324$
Final R indexes [all data]	$R_1 = 0.0262$ $wR_2 = 0.0348$
Largest peak/hole [eÅ ⁻³]	1.10/-0.95

BIDIPY-2-Cl

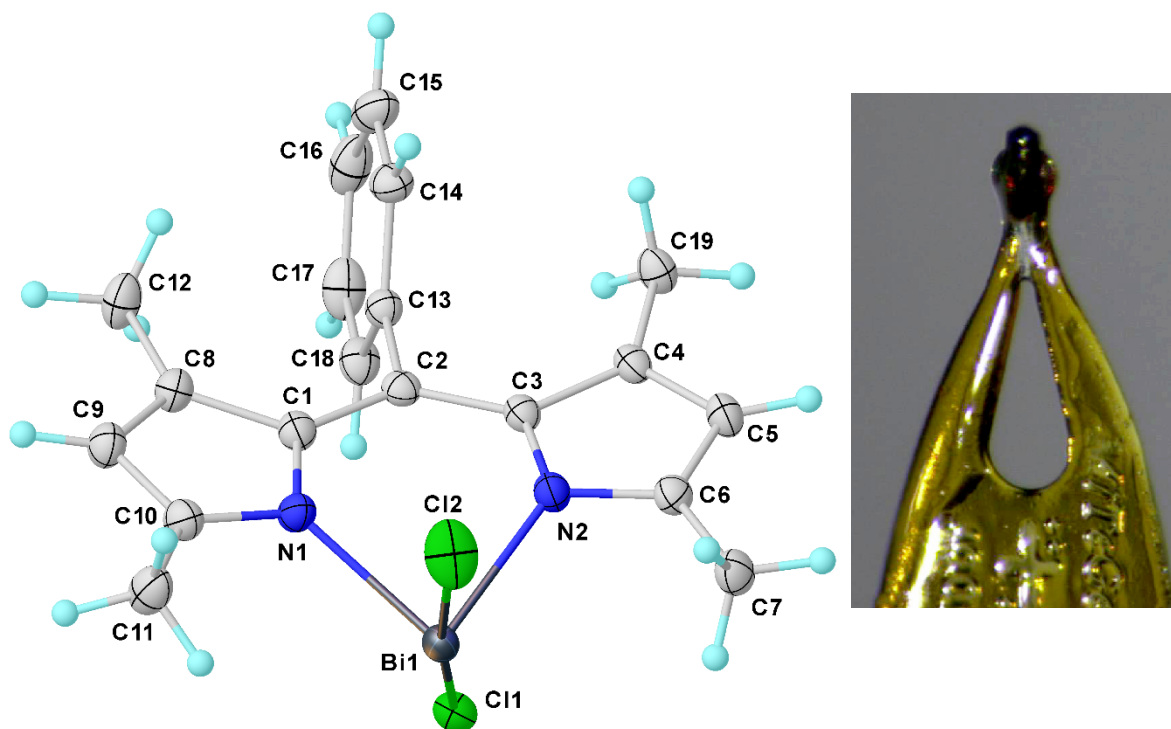


Figure 44: Full asymmetric unit and labeling scheme for **BIDIPY-2-Cl**. Displacement ellipsoids are drawn at 50% probability level. The crystals were obtained from a mixture of THF and hexane.

CCDC number	2241586
Empirical formula	C ₁₉ H ₁₉ BiCl ₂ N ₂
Formula weight	555.24
Temperature [K]	100.00
Crystal system	tetragonal
Space group (number)	<i>I</i> 4 ₁ / <i>a</i> (88)
<i>a</i> [Å]	22.9835(6)
<i>b</i> [Å]	22.9835(6)
<i>c</i> [Å]	14.1686(4)
α [°]	90

β [°]	90
γ [°]	90
Volume [Å ³]	7484.4(4)
<i>Z</i>	16
ρ_{calc} [gcm ⁻³]	1.971
μ [mm ⁻¹]	9.711
<i>F</i> (000)	4224
Crystal size [mm ³]	0.289×0.114×0.056
Crystal colour	dark green
Crystal shape	block

Radiation	MoK α ($\lambda=0.71073$ Å)
2 θ range [°]	4.90 to 63.02 (0.68 Å)
Index ranges	-33 \leq h \leq 33 -33 \leq k \leq 33 -20 \leq l \leq 20
Reflections collected	112176
Independent reflections	6239 $R_{\text{int}} = 0.0366$ $R_{\text{sigma}} = 0.0126$
Completeness to $\theta = 25.242^\circ$	99.9%

Data / Restraints / Parameters	6239/0/221
Goodness-of-fit on F^2	1.049
Final R indexes [$\geq 2\sigma(I)$]	$R_1 = 0.0187$ $wR_2 = 0.0438$
Final R indexes [all data]	$R_1 = 0.0221$ $wR_2 = 0.0452$
Largest peak/hole [$\text{e}\text{\AA}^{-3}$]	1.64/-0.87

BIDIPY-3-Cl

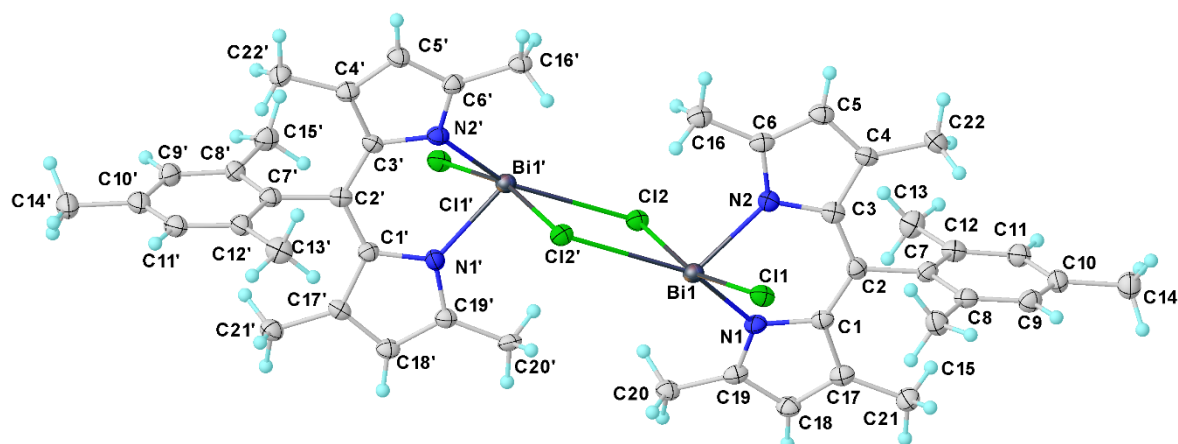
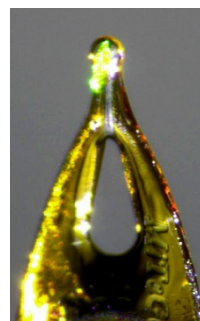


Figure 45: Full asymmetric unit ($Z' = 2$) and labeling scheme for **BIDIPY-3-Cl**.

Displacement ellipsoids are drawn at 30% probability level. The crystals were obtained from a mixture of THF and hexane. Non-merohedral twinning was found for all crystals of this compound that caused problems due to a high ratio of overlapping reflections. Manual optimization of integration parameters (integration box size and minimal common volume) was necessary to obtain acceptable raw data, but still causing considerable residual density artifacts. The two domains were related by the



transformation matrix $(0\ 0\ 1 / -1\ 0\ 0 / 0\ -1\ -0.660)$ and the batch scale factor was refined to 0.2754(7). The $Z' = 2$ situation with no significant alteration in geometry may raise the assumption that the true unit cell is only half the size. However, a cell indexation of a smaller unit cell is only possible under omission of obviously present reflections, hence this unit cell is believed to be correct one. Exploring the structural features reveals the reason for this is the central subunit Bi1–Cl2–Bi1'–Cl2' not being perfectly symmetric, in contrast to the situation of the previous compounds.

CCDC number	2241587
Empirical formula	$C_{22}H_{25}BiCl_2N_2$
Formula weight	597.32
Temperature [K]	100.00
Crystal system	monoclinic
Space group (number)	$P2_1/n$ (14)
a [Å]	7.7393(7)

b [Å]	15.609(2)
c [Å]	36.440(5)
α [°]	90
β [°]	93.984(3)
γ [°]	90
Volume [Å ³]	4391.5(10)
Z	8

ρ_{calc} [gcm ⁻³]	1.807
μ [mm ⁻¹]	8.282
$F(000)$	2304
Crystal size [mm ³]	0.186×0.081×0.021
Crystal colour	yellow
Crystal shape	plate
Radiation	MoK α ($\lambda=0.71073$ Å)
2 θ range [°]	4.26 to 57.45 (0.74 Å)
Index ranges	-10 ≤ h ≤ 10 0 ≤ k ≤ 21 0 ≤ l ≤ 49
Reflections collected	11478
Independent reflections	11478 $R_{\text{int}} = ?$ $R_{\text{sigma}} = 0.0299$
Completeness to $\theta = 25.242^\circ$	99.4%
Data / Restraints / Parameters	11478/0/502
Goodness-of-fit on F^2	1.064
Final R indexes [$I \geq 2\sigma(I)$]	$R_1 = 0.0464$ $wR_2 = 0.1047$
Final R indexes [all data]	$R_1 = 0.0519$ $wR_2 = 0.1090$

Largest peak/hole [eÅ ⁻³]	1.91/-3.56
---------------------------------------	------------

9. References

- [1] N. A. Yakelis, R. G. Bergman, *Organometallics* **2005**, *24*, 3579–3581.
- [2] S. L. Yutanova, M. B. Berezin, A. S. Semeikin, E. V. Antina, G. B. Guseva, A. I. V'Yugin, *Russ. J. Gen. Chem.* **2013**, *83*, 545–551.
- [3] J. L. Sessler, L. R. Eller, W. S. Cho, S. Nicolaou, A. Aguilar, J. T. Lee, V. M. Lynch, D. J. Magda, *Angew. Chem. Int. Ed.* **2005**, *44*, 5989–5992.
- [4] X. Liu, H. Nan, W. Sun, Q. Zhang, M. Zhan, L. Zou, Z. Xie, X. Li, C. Lu, Y. Cheng, *Dalt. Trans.* **2012**, *41*, 10199–10210.
- [5] J. Karges, O. Blacque, H. Chao, G. Gasser, *Inorg. Chem.* **2019**, *58*, 12422–12432.
- [6] C. Yu, P. Zhang, F. Gao, S. Zhang, X. Li, *Polym. Chem.* **2018**, *9*, 603–610.
- [7] A. A. S. Ali, J. Cipot-Wechsler, S. M. Crawford, O. Selim, R. L. Stoddard, T. S. Cameron, A. Thompson, *Can. J. Chem.* **2010**, *88*, 725–735.
- [8] L. Cunha Dias De Rezende, M. Menezes Vaidergorn, J. C. Biazotto Moraes, F. Da Silva Emery, *J. Fluoresc.* **2014**, *24*, 257–266.
- [9] S. Grimme, A. Hansen, S. Ehlert, J. M. Mewes, *J. Chem. Phys.* **2021**, *154*, 064103.
- [10] F. Neese, F. Wennmohs, U. Becker, C. Riplinger, *J. Chem. Phys.* **2020**, *152*, 224108.
- [11] L. Goerigk, S. Grimme, *J. Chem. Phys.* **2010**, *132*, 184103.
- [12] F. Weigend, R. Ahlrichs, *Phys. Chem. Chem. Phys.* **2005**, *7*, 3297–3305.
- [13] G. M. Sheldrick, *Acta Crystallogr. Sect. A Found. Crystallogr.* **2008**, *64*, 112–122.
- [14] O. V. Dolomanov, L. J. Bourhis, R. J. Gildea, J. A. K. Howard, H. Puschmann, *J. Appl. Crystallogr.* **2009**, *42*, 339–341.
- [15] D. Kratzert, *FinalCif, V113*, can be found under <https://dkratzert.de/finalcif.html>.
- [16] T. Kottke, D. Stalke, *J. Appl. Crystallogr.* **1993**, *26*, 615–619.
- [17] C. Liu, Y. Dai, Q. Han, C. Liu, Y. Su, *Chem. Commun.* **2023**, *59*, 2161–2164.
- [18] S. Alvarez, *Dalt. Trans.* **2013**, *42*, 8617–8636.